Computational Aero-Acoustics Analysis of the Broadband Engine Noise Simulator Experiment

(presented at 21st AIAA/CEAS Aeroacoustics Conference, Dallas, TX)

Christoph Brehm
Science and Technology Corporation

Jeffrey Housman, Cetin C. Kiris
Applied Modeling and Simulation Branch
NASA Ames Research Center

Florence Hutcheson
Aero-acoustic Branch
NASA Langley Research Center

Funded by the NASA Fundamental Aeronautics Program Environmentally Responsible Aviation (ERA) Project

20th of August, 2015, AMS Seminar Series, NASA Ames Research Center

Outline

- Introduction to BENS Aero-Acoustic Analysis
- Computational Simulation Strategy and Setup
- Characterization of Flow Field in Source Region
- Noise Source Identification
  - Causality Method
  - Proper Orthogonal Decomposition (paper only)
- Linear Acoustic Analysis
  - Acoustic Model of FJID
  - BENS Scattering Results
- Conclusions/Outlook

OUTLINE

- Introduction to BENS Aero-Acoustic Analysis
- Computational Simulation Strategy and Setup
- Characterization of Flow Field in Source Region
- Noise Source Identification
  - Causality Method
  - Proper Orthogonal Decomposition (paper only)
- Linear Acoustic Analysis
  - Acoustic Model of FJID
  - BENS Scattering Results
- Conclusions/Outlook

Part 1:
fundamental noise source analysis

Part 2:
applied linear acoustic analysis

Outline

- **Introduction to BENS Aero-Acoustic Analysis**
- Computational Simulation Strategy and Setup
- Characterization of Flow Field in Source Region
- Noise Source Identification
- Linear Acoustic Analysis
  - Acoustic Model of FJID
  - BENS Scattering Results
- Conclusions/Outlook

INTRODUCTION

- Advantage of HWB/BWB is potential to shield noise by main body

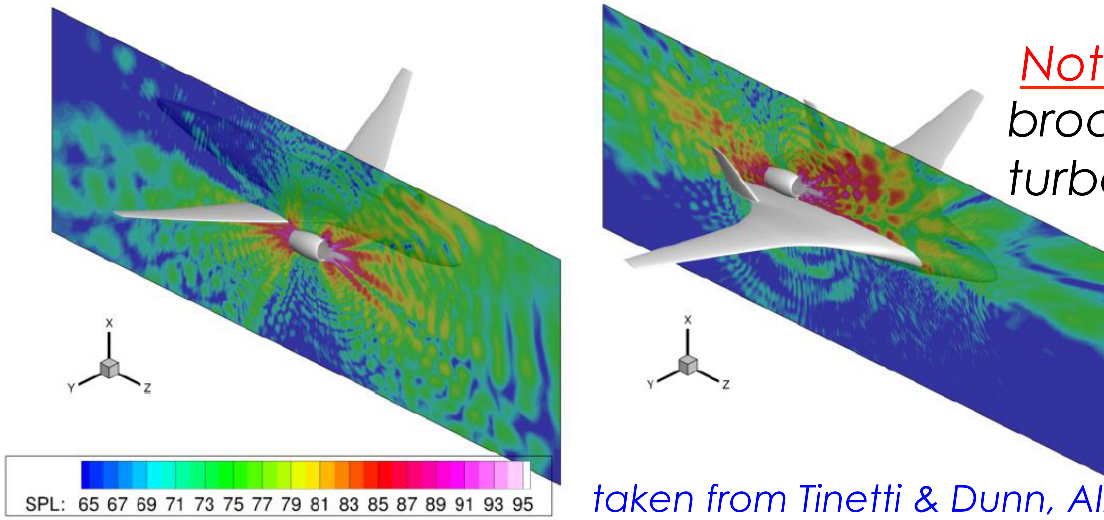

<u>*Note:*</u> *This work focuses on broadband component of turbomachinery noise*

taken from Tinetti & Dunn, AIAA-2012

- Large test matrix for different flight conditions and airplane configurations
- Use **equivalent source method** to solve 3D Helmholtz equation in frequency domain (fast turn-around times) ➔ <u>Linear Acoustic Analysis</u>
  - Incident pressure field can be generated by using analytic source distribution (monopoles, dipoles, and/or quadrupoles)
- Use **CFD** solver to develop simplified acoustic model (or sample on permeable surface) ➔ <u>LES of Nonlinear Source Region</u>
- Improved **understanding of noise generation process** guides the development of acoustic model ➔ <u>Noise Source Identification</u>

Overview of BENS CAA Strategy

Objective: Develop fully predictive BENS-CAA capability

1.) High fidelity CFD simulation of FJID & development of linear acoustic model

Four Jet Impingement Device (FJID) used as broadband noise source

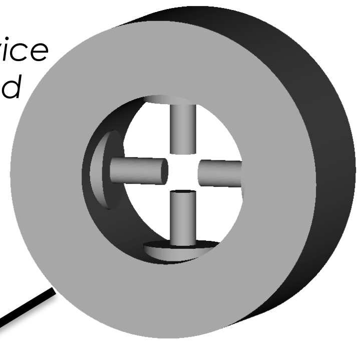

2.) BENS experiment by Hutcheson et. al. [2014]

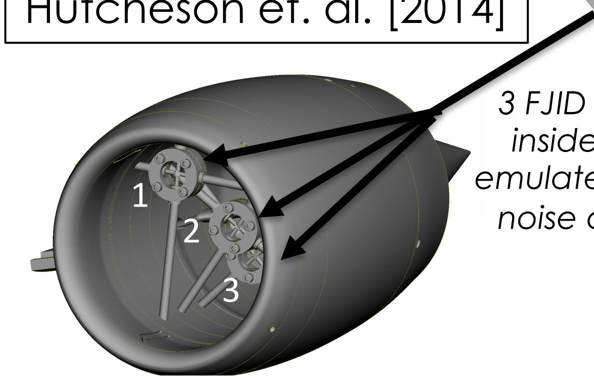

3 FJID are placed inside engine to emulate broadband noise component

3.) Linear acoustic Analysis of BENS experiment using FJID model

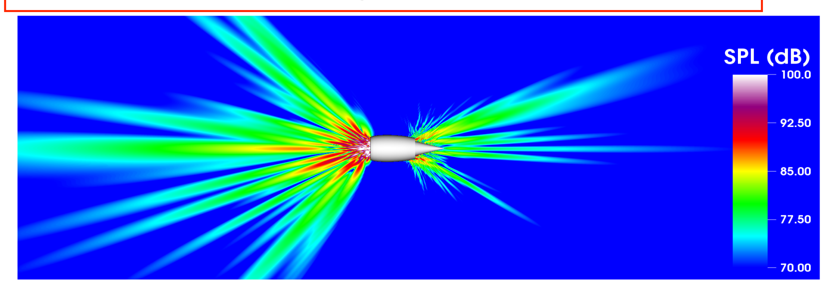

5.) Engine placement study is performed using experiment and CAA

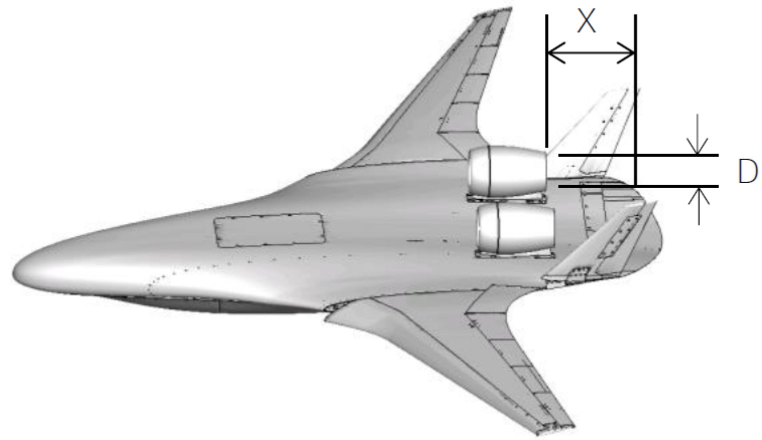

4.) Comparison of BENS acoustic model with experimental data from Hutcheson et al. [2014]

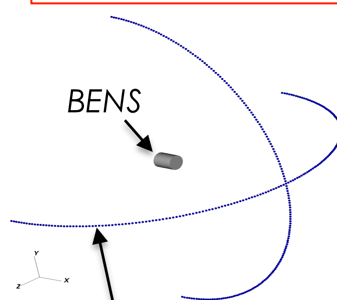

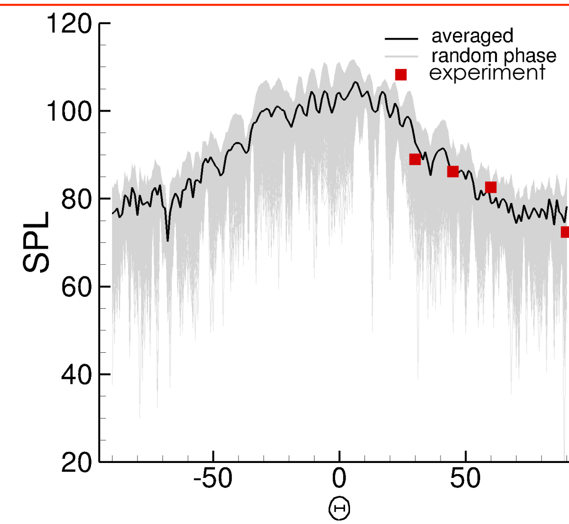

Launch Ascent & Vehicle Aerodynamics (LAVA) Framework

LAVA is being developed at NASA Ames Research Center

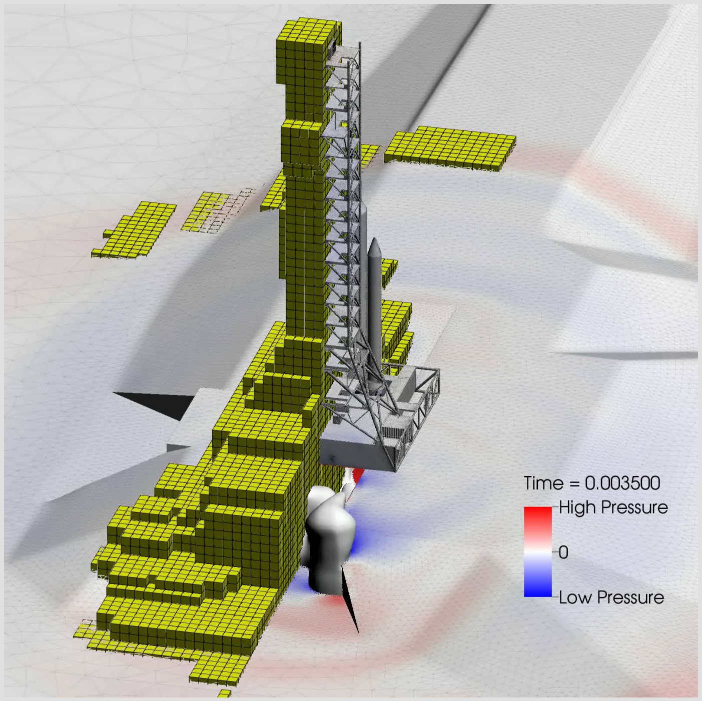

Cartesian AMR
- Essentially no manual grid generation
- Highly efficient Adaptive Mesh Refinement (AMR)
- Low computational cost
- Reliable higher order methods are available
- Non-body fitted -> Resolution of boundary layers problematic/ inefficient

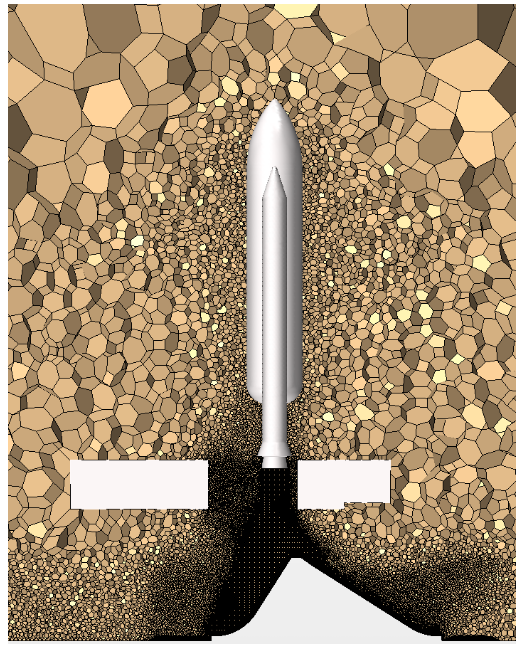

Unstructured Arbitrary Polyhedral
- Grid generation is mostly automated
- Body fitted grids
- Grid quality can be questionable
- High computational cost
- Higher order methods are yet to fully mature

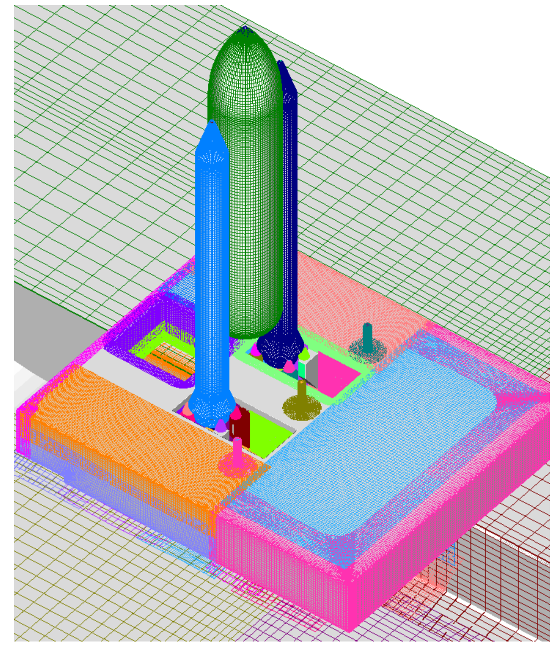

Overset Structured Curvilinear
- High quality, body fitted grids
- Low computational cost
- Reliable higher order methods are available
- Grid generation is largely manual and time consuming

*Kiris et al.(2014), Sozer et al. (2014), Brehm et al. (2014)

Outline

- Introduction to BENS Aero-Acoustic Analysis
- **Computational Simulation Strategy and Setup**
- Characterization of Flow Field in Source Region
- Noise Source Identification
- Linear Acoustic Analysis
  - Acoustic Model of FJID
  - BENS Scattering Results
- Conclusions/Outlook

Precursor Simulation

Precursor simulation to obtain FJID nozzle exit conditions

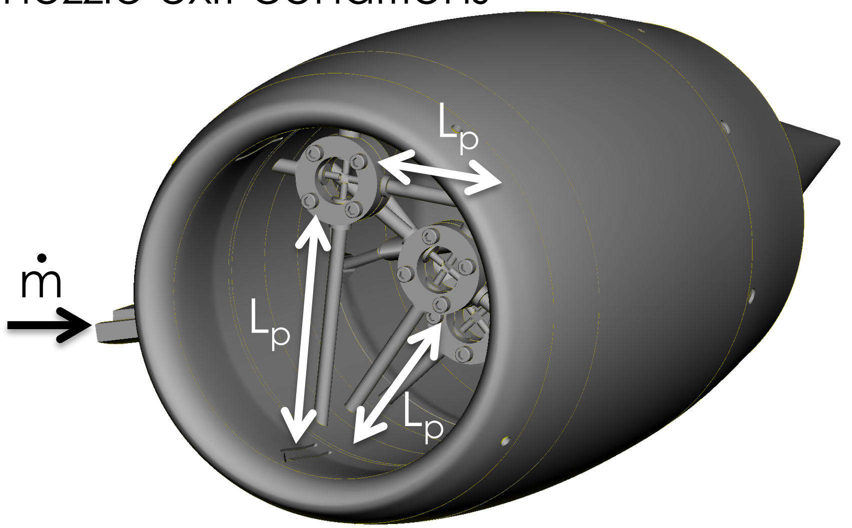

Mach Number Contours and Sonic Line

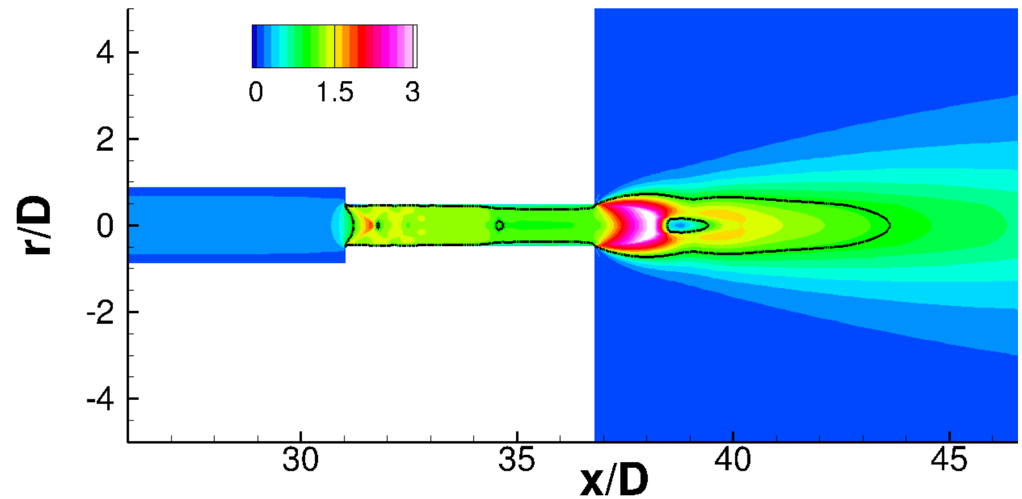

- Precursor simulation with LAVA-Unstructured (assuming symmetry)
- Match mass-flow rate in experiment
- Use averaged pipe length, L_p
- Extract boundary conditions at the nozzle exit
- Reference conditions are based on mean exit conditions: p_{ref}=1atm, V_{ref}=335.8 m/s, and T_{ref} =235.3K, Re=75,000

Nozzle Exit Boundary Conditions

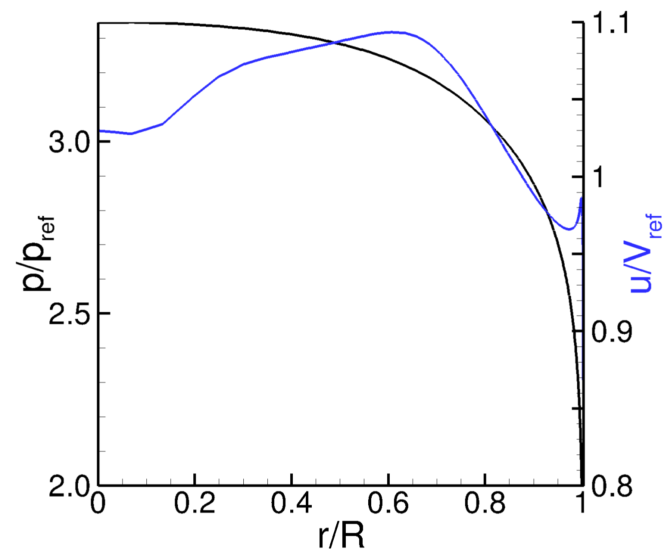

FJID Simulation Setup

Four-Jet-Impingement Device (FJID)

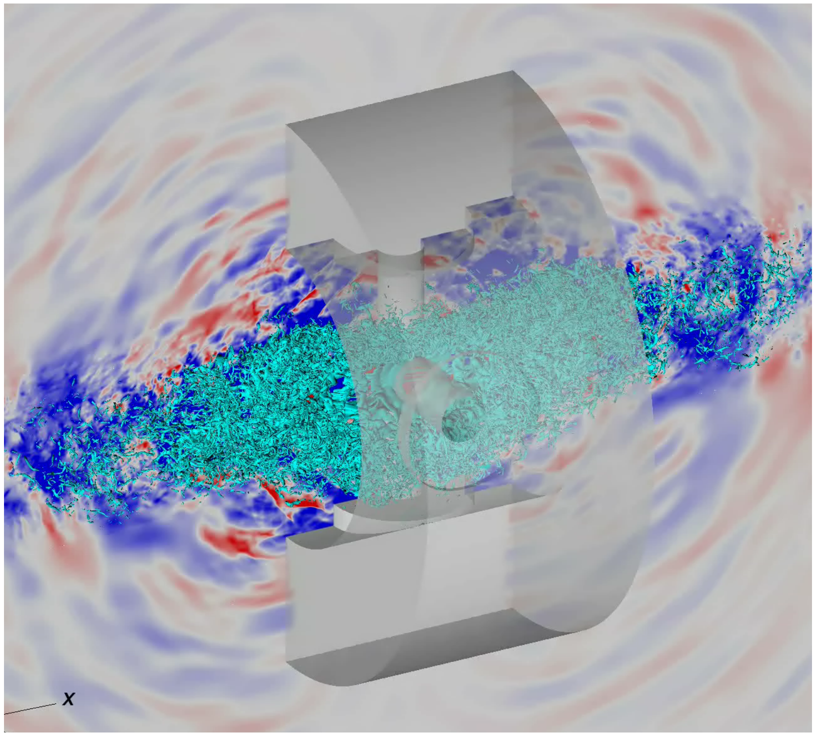

High Frequency Sampling on Planes

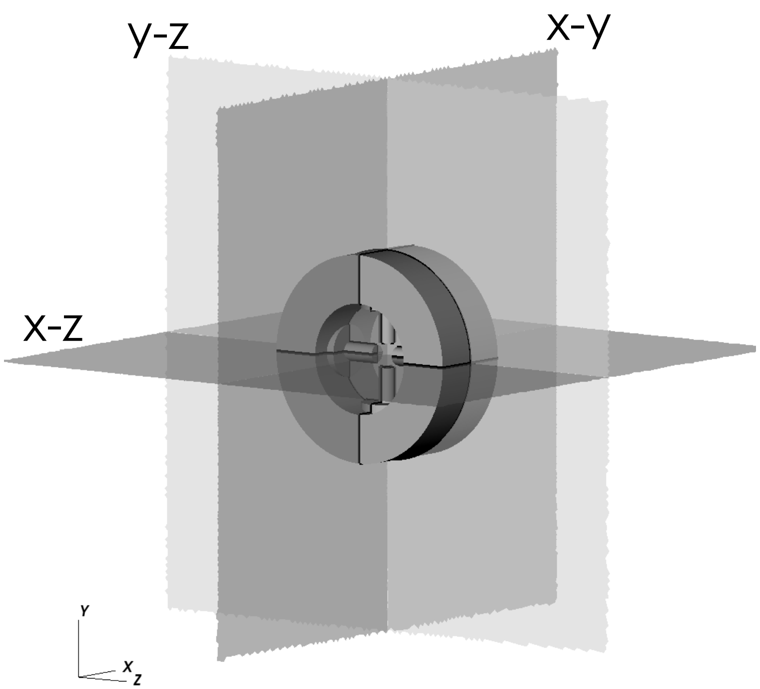

- Higher-order shock capturing scheme: modified ZWENO5/6
- 4th-order explicit Runge-Kutta time-integration with Δt defined through CFL≈0.5
- Implicit large eddy simulation based on previous experience with jet impingement problem
- Immersed boundary method (no wall modeling approach employed)

Validation of Simulation Strategy

- A large eddy simulation (LES) approach is necessary because DNS is not feasible for current flow conditions
- Simulation strategy with respect to nozzle inflow conditions and sub-grid scale modeling is aligned with recommendations of Shur *et al.* [2005a,b]
- Used modified WENO-6 scheme (Hu et. [2010] and Brehm et al. [2013,2015])
  - Hu & Adams [2011] demonstrated superior physically motivated scale separation properties of modified WENO-6
- No inflow forcing needed because impinging jet generates elevated background noise level; eliminates dependence on free parameters

Comparison with Experimental Data

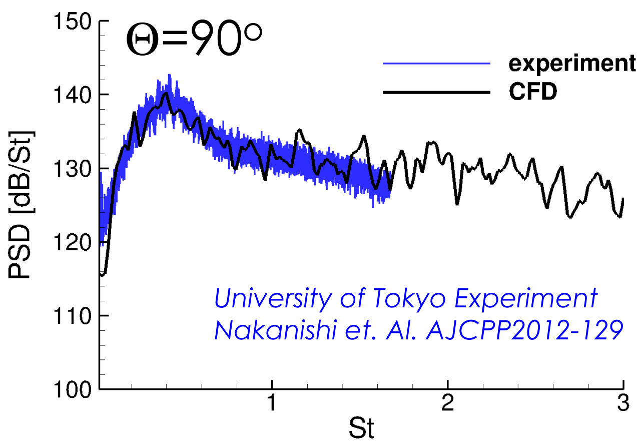

Brehm, Housman, & Kiris (2013 & 2015)

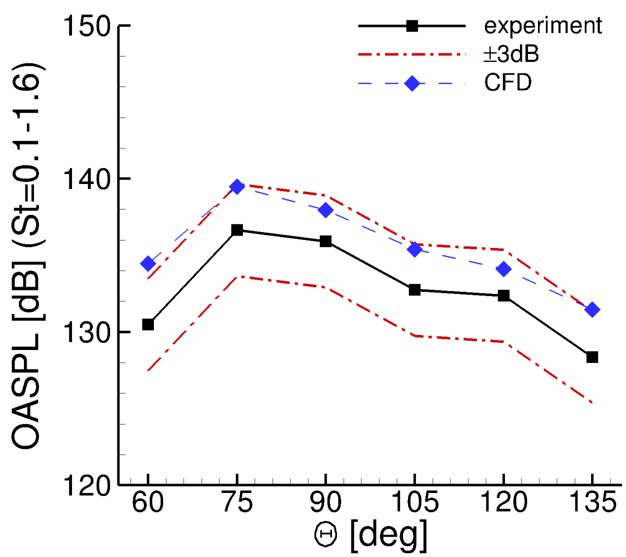

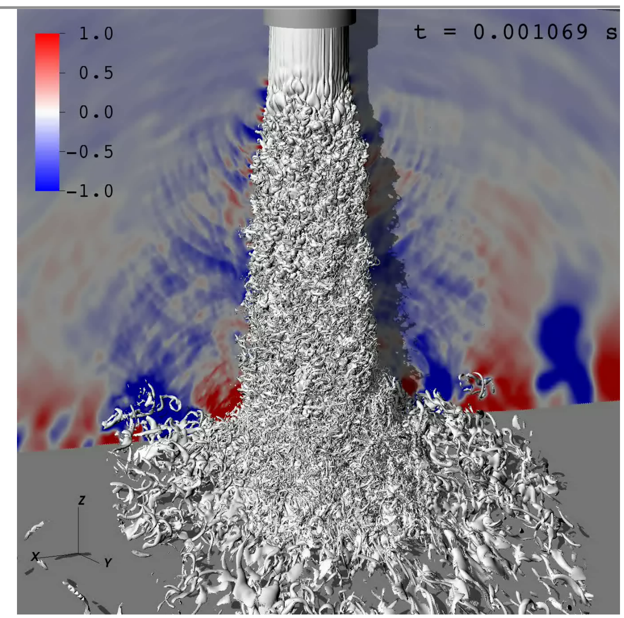

Computational Mesh

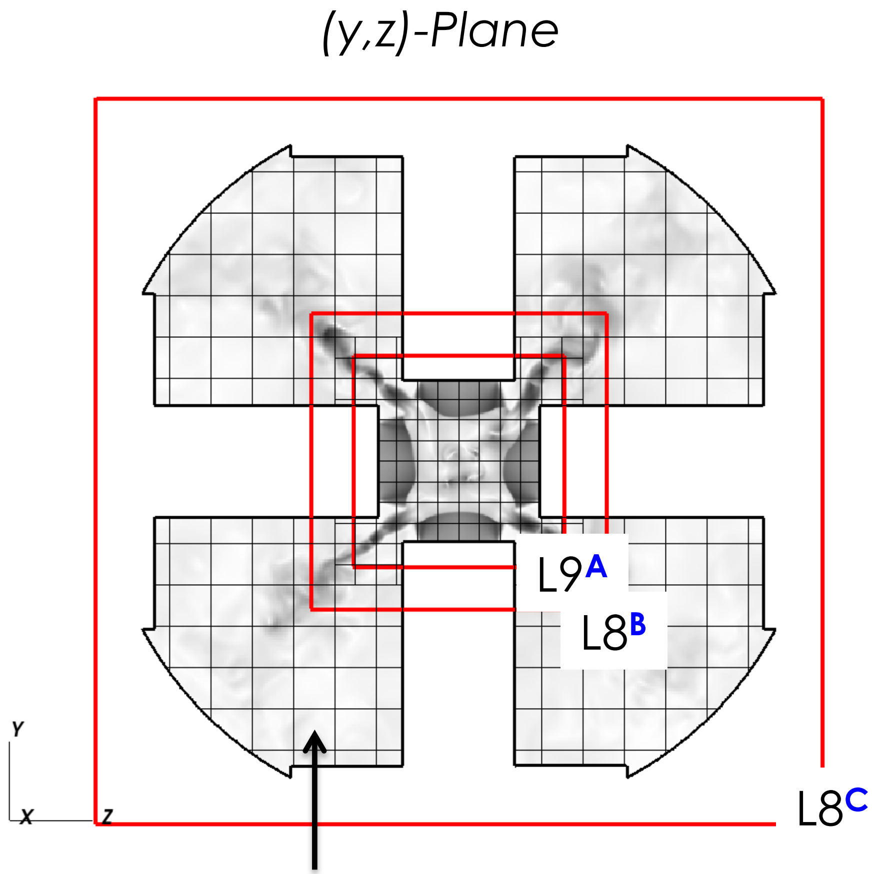

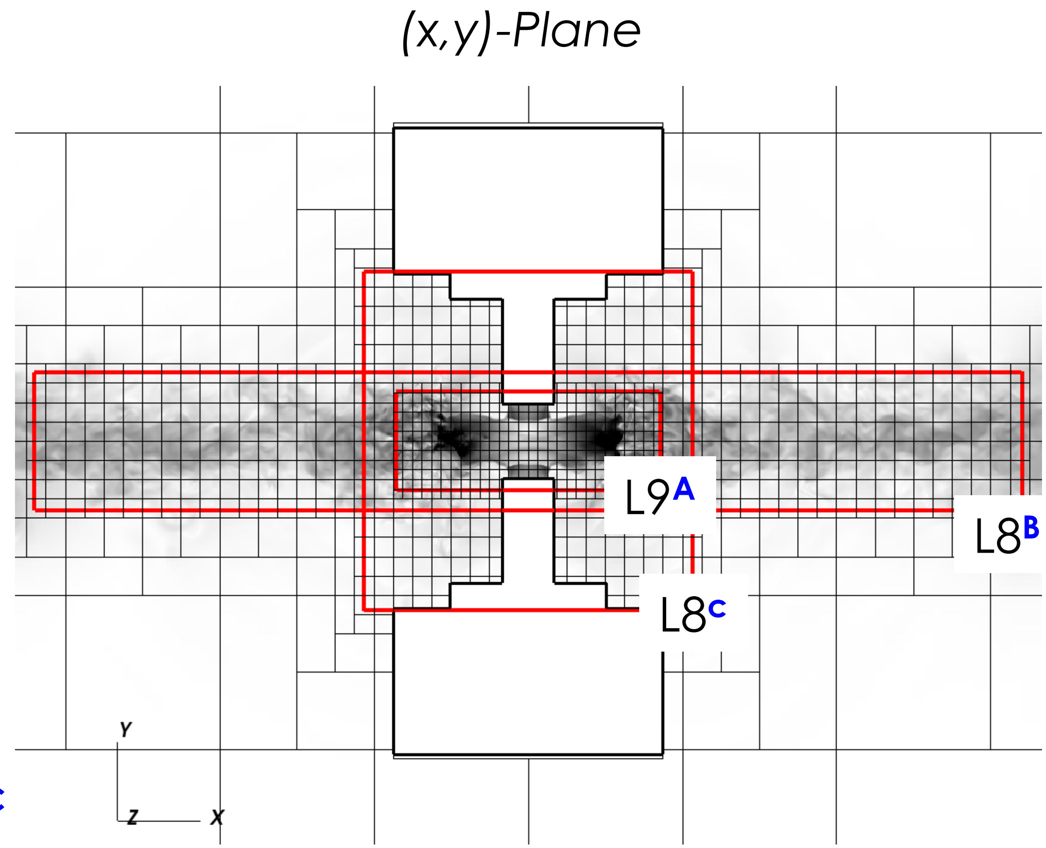

note, each box contains 16^3 grid points

- three grid resolutions ($\approx 100\times10^6$, 180×10^6, and 300×10^6)
- Three refinement boxes (levels 9 and 8)
- Factor 2 refinement

A. Coarse: 100×10^6 grid points (Δx_{min}=3.6e-5, 56 points/D)

B. Medium: 180×10^6 grid points (Δx_{min} =2.4e-5, 83 points/D)

C. Fine: 300×10^6 grid points (Δx_{min} =1.8e-5, 112 points/D)

OUTLINE

- Introduction to BENS Aero-Acoustic Analysis
- Computational Simulation Strategy and Setup
- **Characterization of Flow Field in Source Region**
- Noise Source Identification
- Linear Acoustic Analysis
  - Acoustic Model of FJID
  - BENS Scattering Results
- Conclusions/Outlook

Flow Visualization

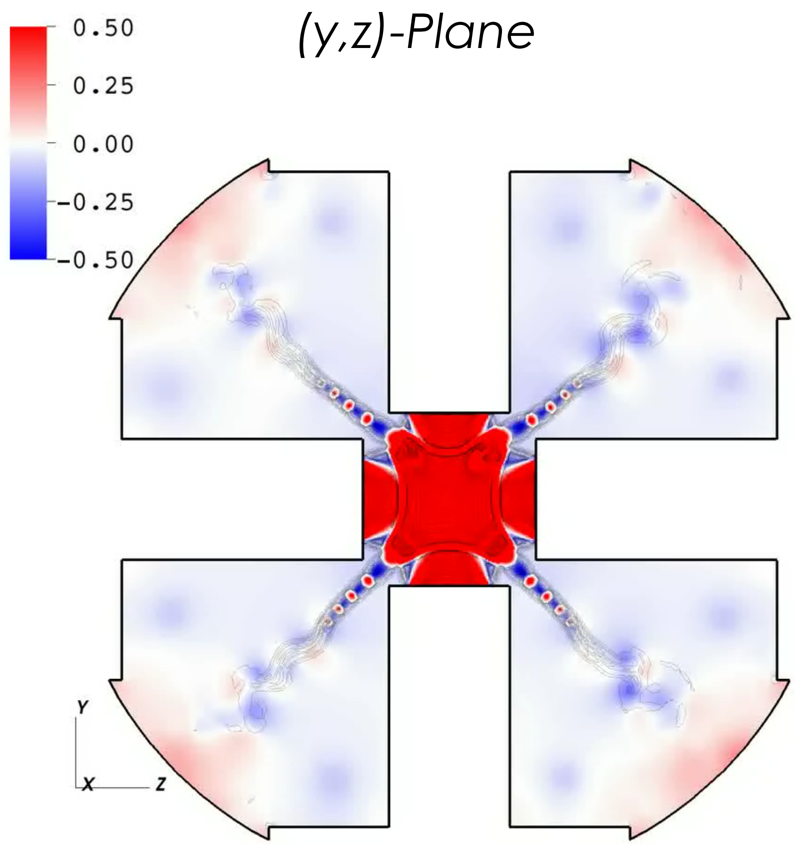

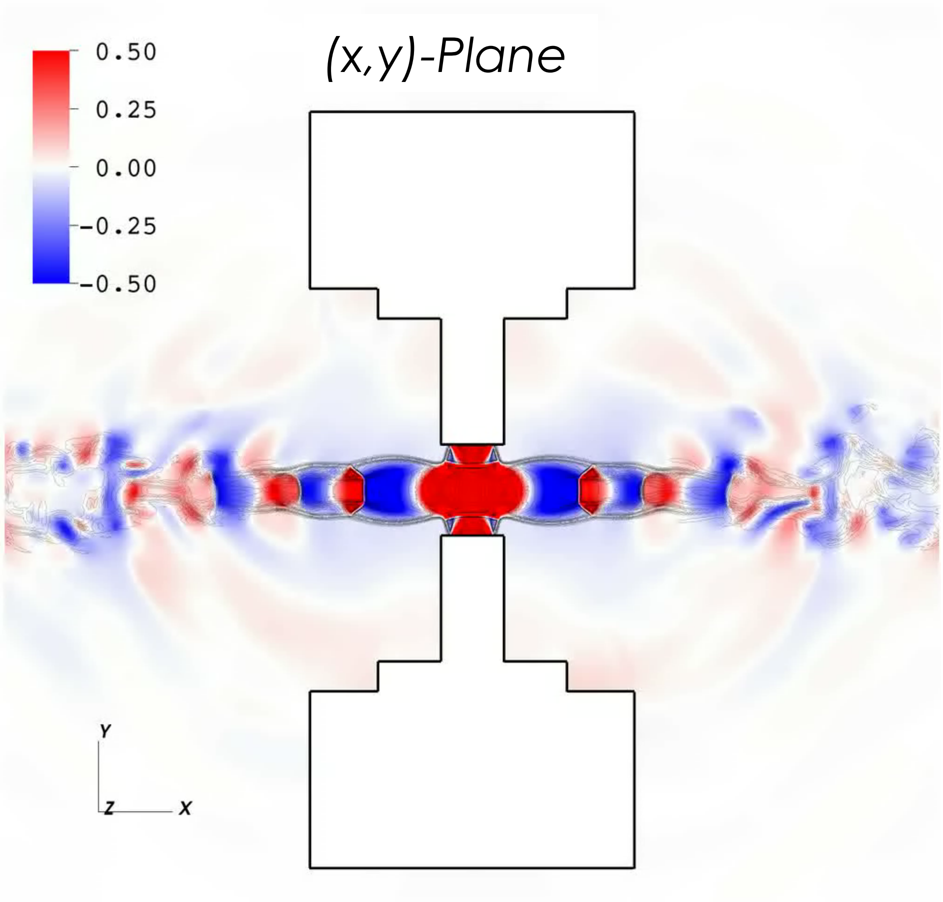

Gauge Pressure (in atm) and contour lines of |Grad(ρ)|

FJID CFD Simulation

Gauge Pressure (in atm) and Mach number contours

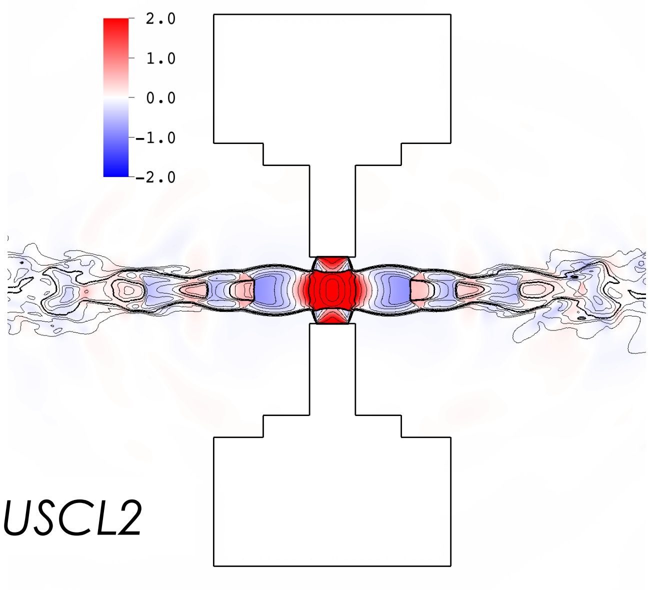

MUSCL2

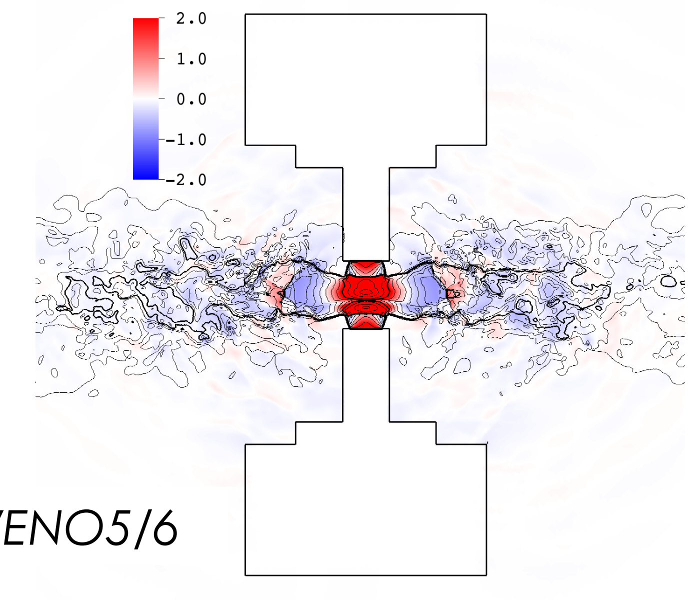

WENO5/6

Addressing CFD challenges for harsh FJID flow conditions:

- Strong longitudinal vortices generate localized low pressure regions
- Challenging for higher-order CFD methods
- Different numerical schemes were used: various numerical fluxes, different implementations of the WENO scheme, implicit and explicit time-integration
- Robustness issue of WENO scheme was addressed
- Most robust version, i.e. MUSCL2, requires a large amount of grid points

Time-Averaged Flow Field

Gauge Pressure (in atm) and Mach number contours

(y,z)-Plane

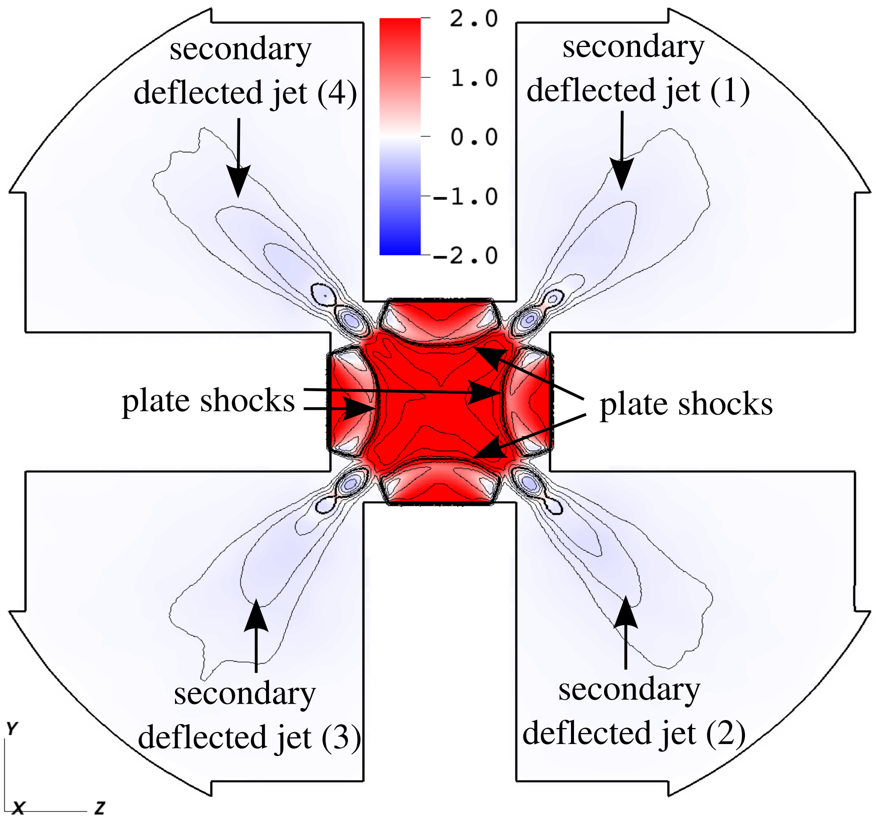

(x,z)-Plane

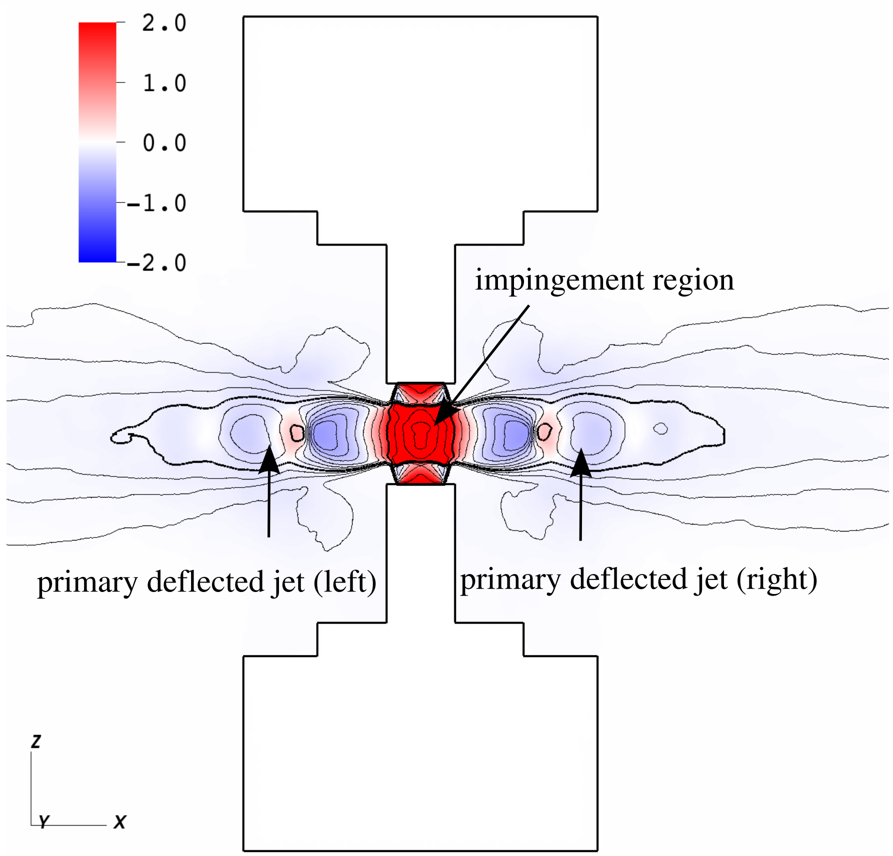

- Expected that two jets in x-direction are main contributors to acoustic noise generation

Grid Resolution Study

Power Spectral Energy for Pressure

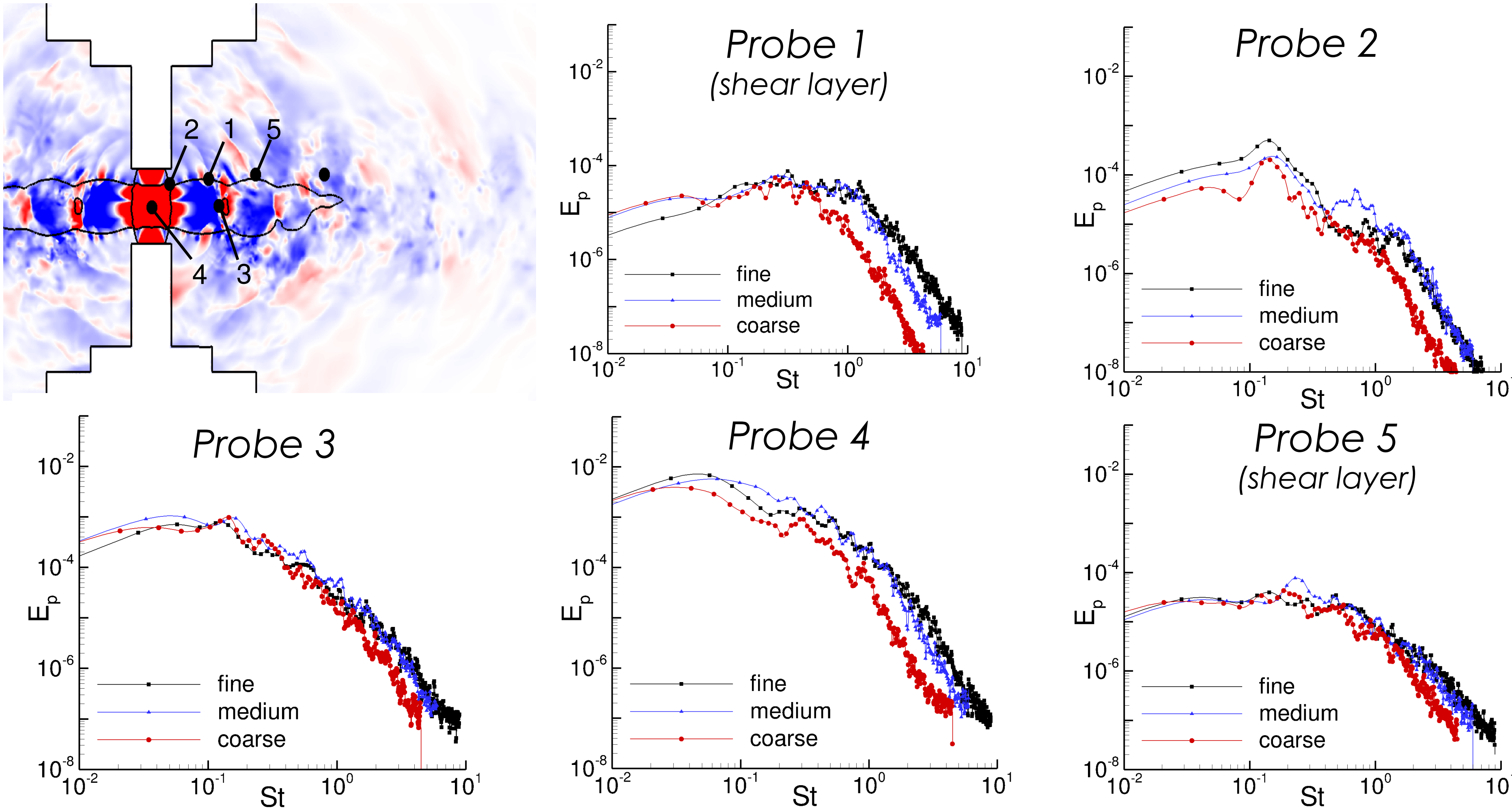

- Good grid convergence for power spectral energy of pressure
- Flat broadband peak in shear-layer (probes 1 & 5)
- Lower frequencies in impingement region and first shock diamond (probes 3 & 4)

Reynolds-Stresses

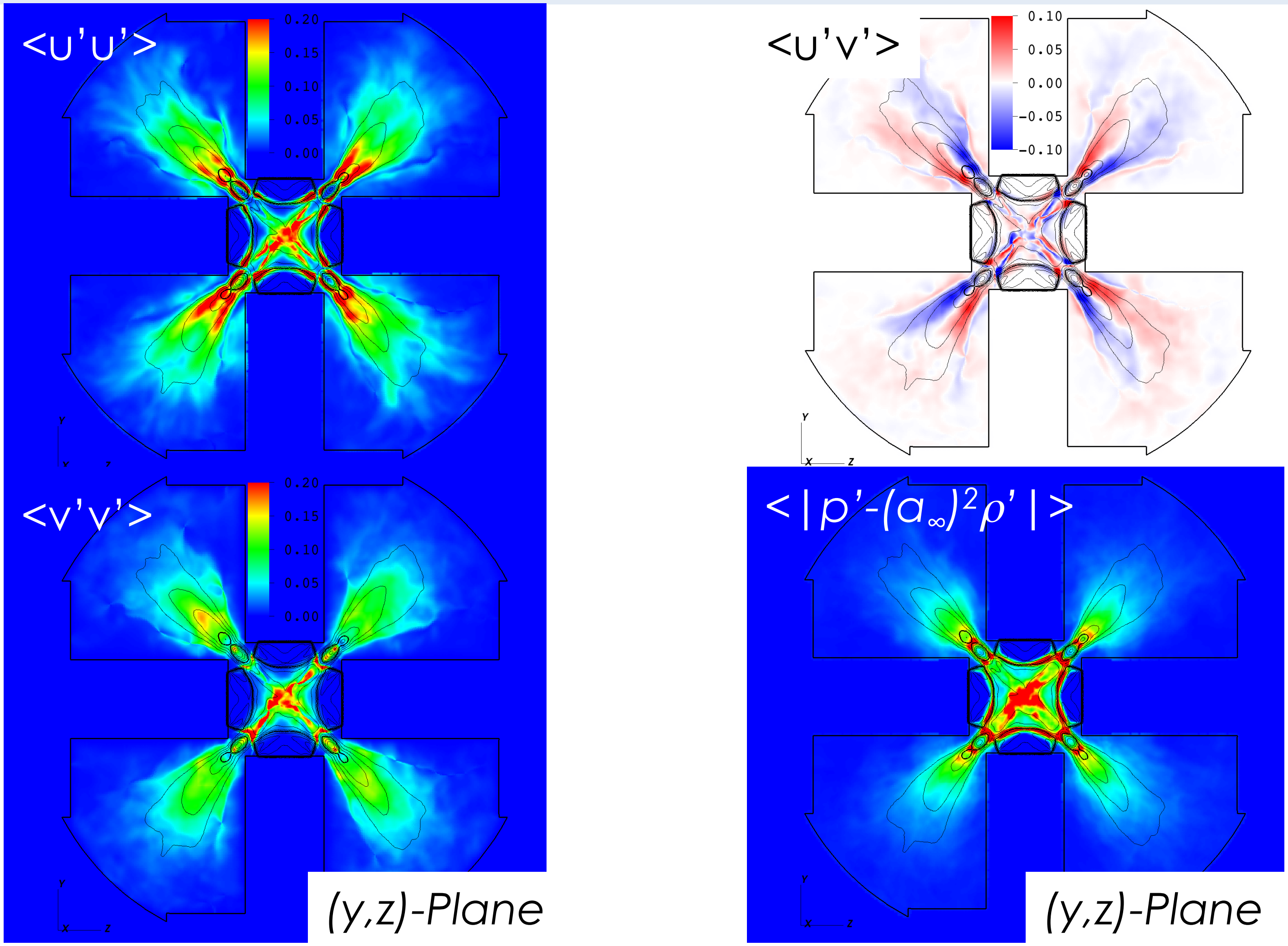

- Reynolds stresses provide an idea about regions with large unsteadiness but does not account for radiating part of the solution
- Shear-layers and impingement region display large normal Reynolds stresses
- <u'v'> provides idea about vortical motion in shear-layers

Reynolds-Stresses

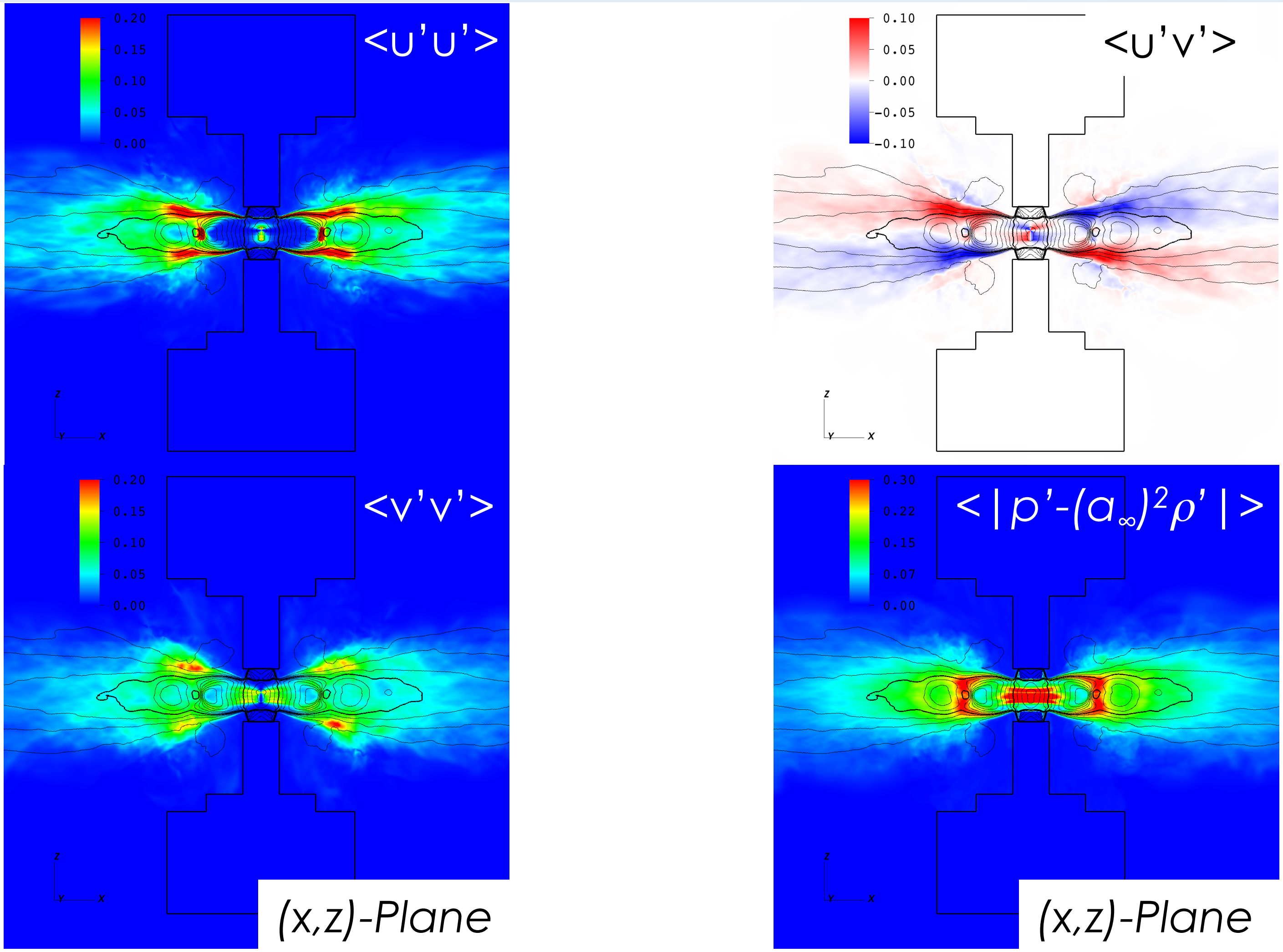

- Large entropy fluctuations in first shock diamond structure and inside impingement region (cannot be obtained with RANS simulation)
- Jet breaks up quickly (unsteadiness concentrated in vicinity of FJID)
- Slightly larger fluctuations in <u’u’> than in <v’v’> in the shear layer

Discrete Wavelet Transform

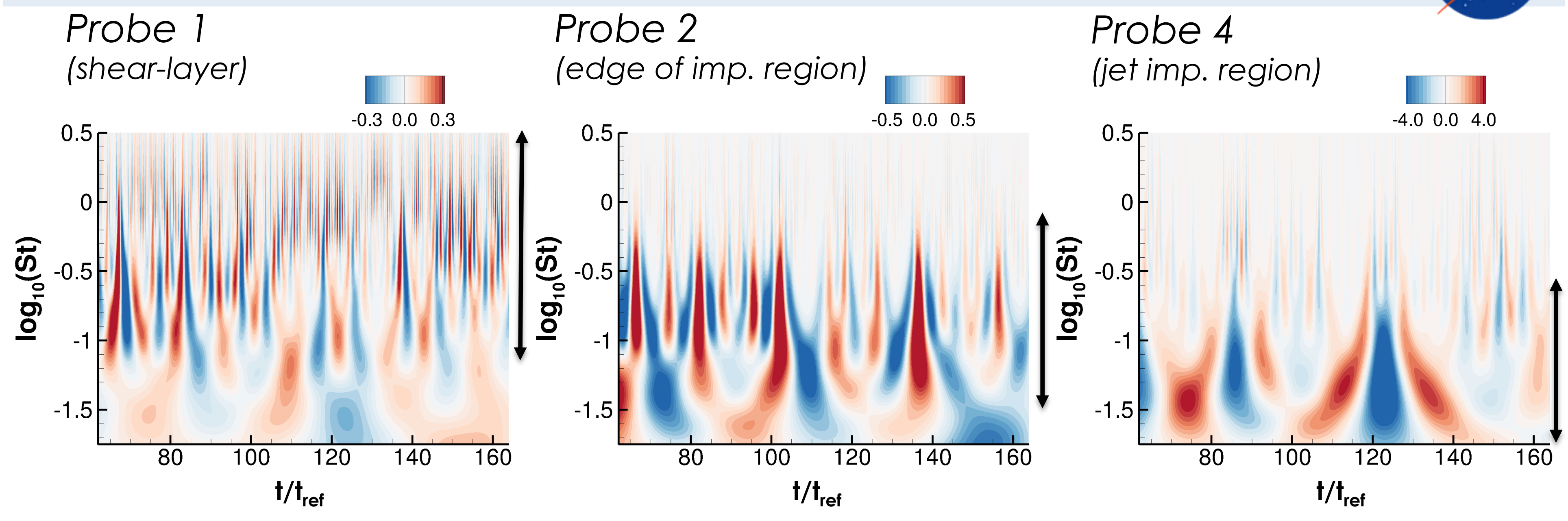

- Using Ricker wavelets
- Pseudo frequency: $\tilde{St} = \dfrac{St_c}{aT_s}$

  with sampling period, T_S, center frequency, St_C, and scale of wavelet, a

Why wavelet transforms?

- DWT offers different view on analyzing unsteady flow field
  - Wavelets captures both frequency & location information
  - Instantaneous DWT spectra are used to study flow physics

Discrete Wavelet Transform

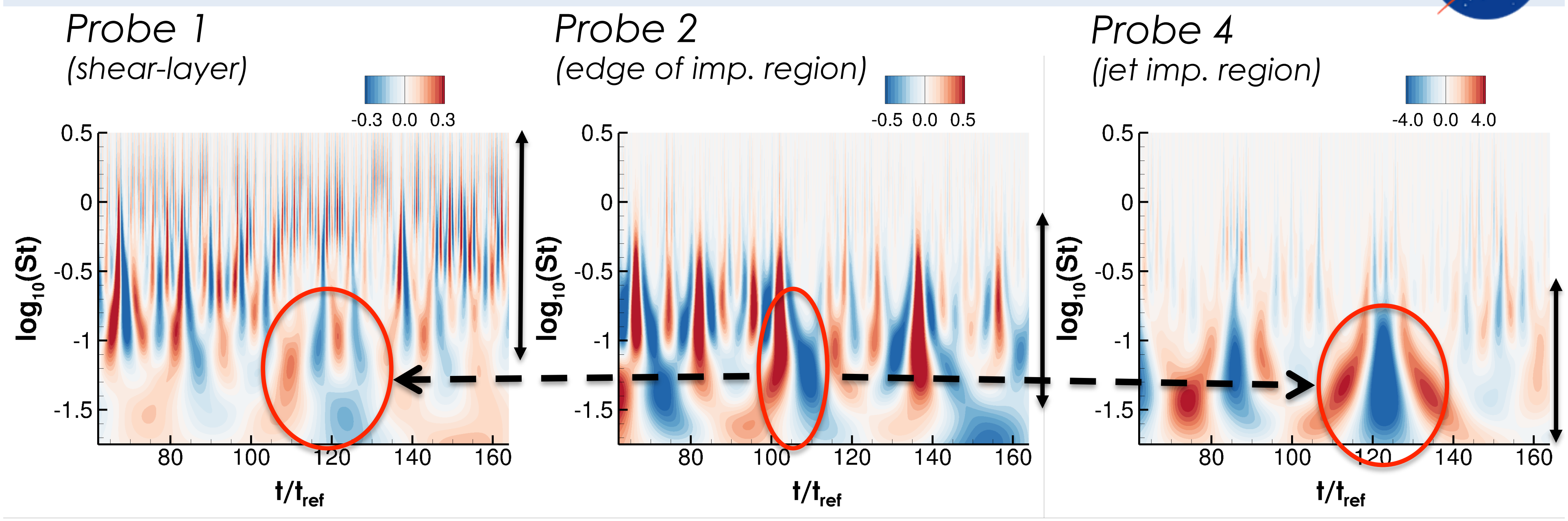

- Using Ricker wavelets
- Pseudo frequency: $\tilde{St} = \dfrac{St_c}{aT_s}$

with sampling period, T_S, center frequency, St_C, and scale of wavelet, a

Why wavelet transforms?

- DWT offers different view on analyzing unsteady flow field
  - Wavelets captures both frequency & location information
  - Instantaneous DWT spectra are used to study flow physics

Discrete Wavelet Transform

Comparison of Fourier spectrum and wavelet pseudo spectrum

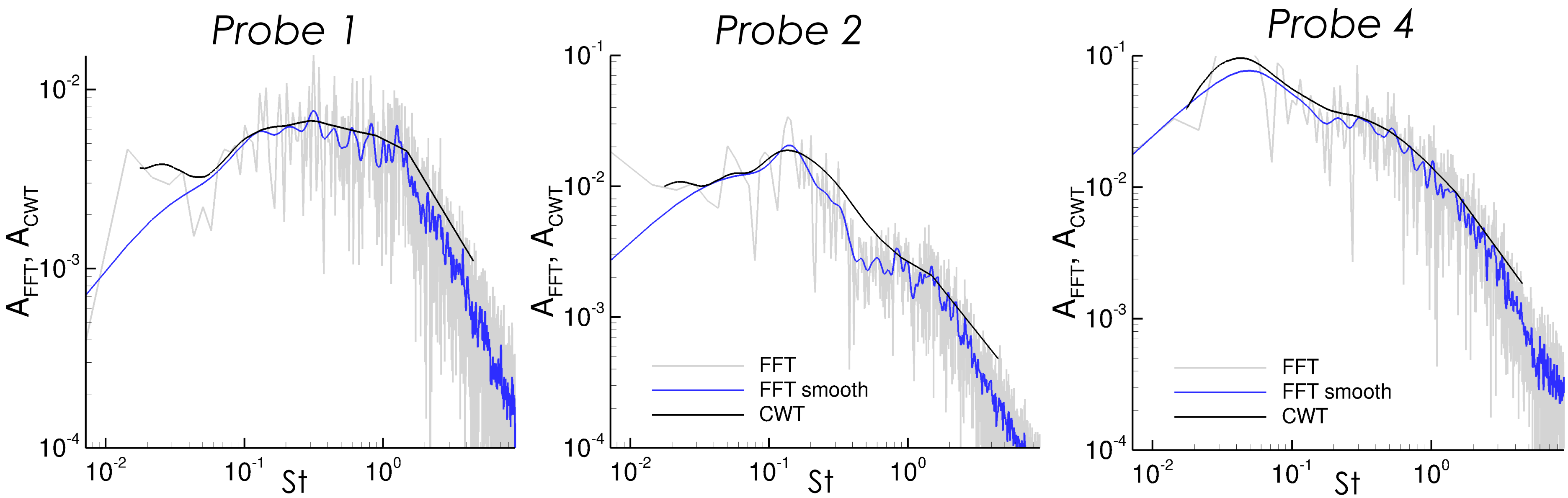

- How does DFT compare to DWT?
- Pseudo spectrum was computed with:

$$A_{DWT}\left(\tilde{S}t\right) = \alpha \sqrt{\frac{\int_{t_1}^{t_2} A^2\left(\tilde{S}t, t\right) dt}{t_2 - t_1}}$$

- General trends between Fourier transform and wavelet transforms match well
- Pseudo frequency scaling allows straightforward interpretation

Wavelet Transform

Wavelet Transformed Time-Signals

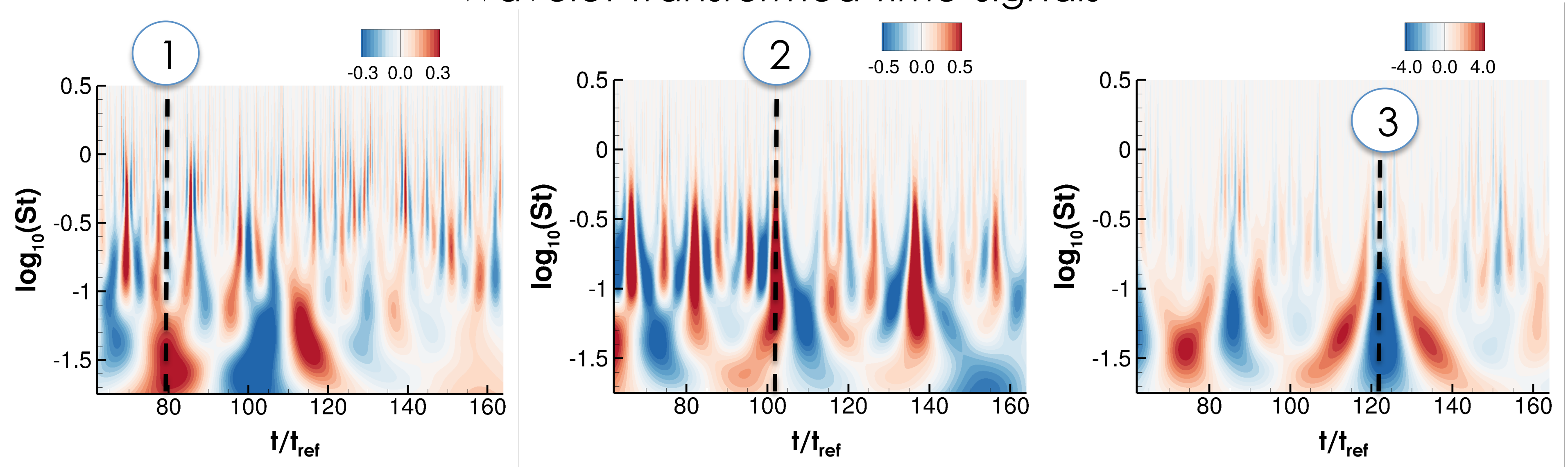

Instantaneous Snapshots of Gauge Pressure and Dilatation Contour Lines

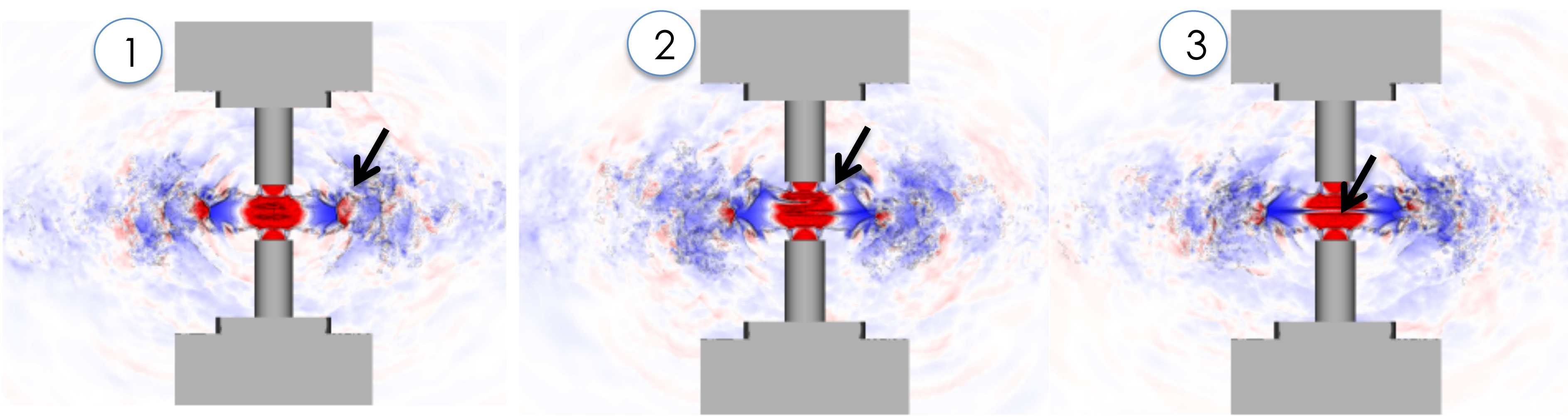

- Highly intermittent flow field

Intermittency

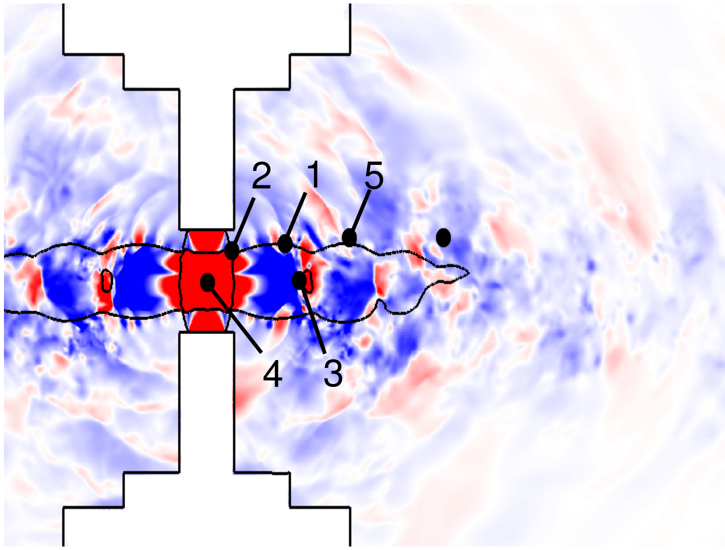

- Flow field is highly intermittent
- Definition $I(t) = \begin{cases} 1 & \text{if } q < 0.5\langle q \rangle \\ 0 & \text{otherwise.} \end{cases}$

  with $q=0.5(u'^2+v'^2+w'^2)$ and $q=p'^2$
- Intermittency factor, $\gamma = \langle I(t) \rangle$
- Laminar/turbulent: $\gamma \approx 0$ and intermittent $\gamma \approx 1$

Probe 2

(high intermittency in $E_{k'}$)

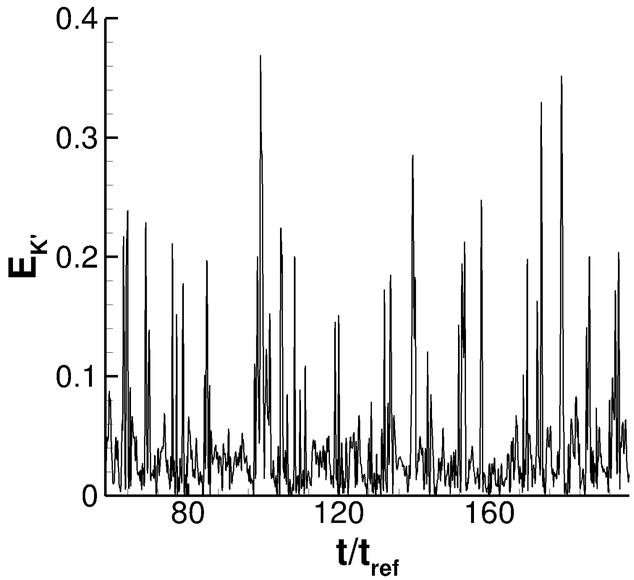

Probe 1

(low intermittency in $(p')^2$)

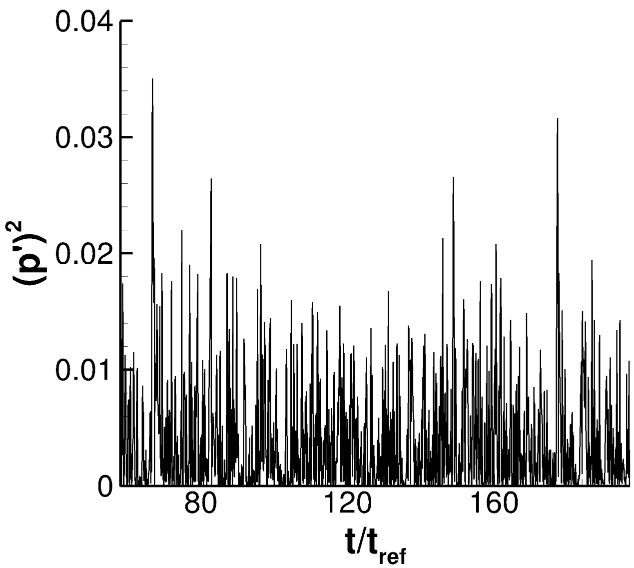

Probe 3

(high intermittency in $(p')^2$)

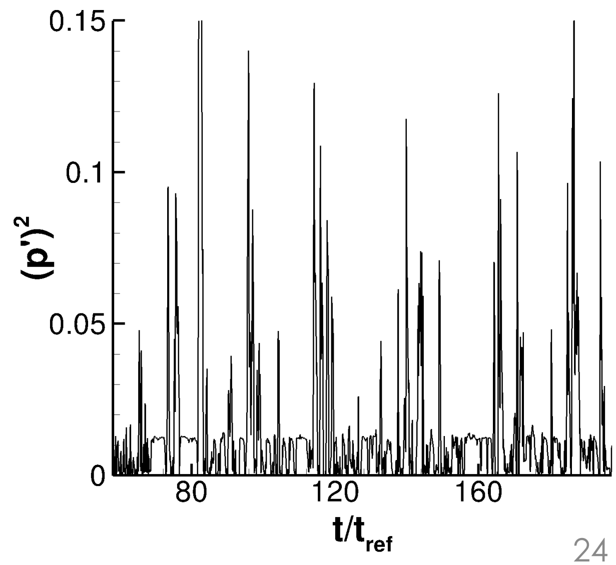

Intermittency Maps

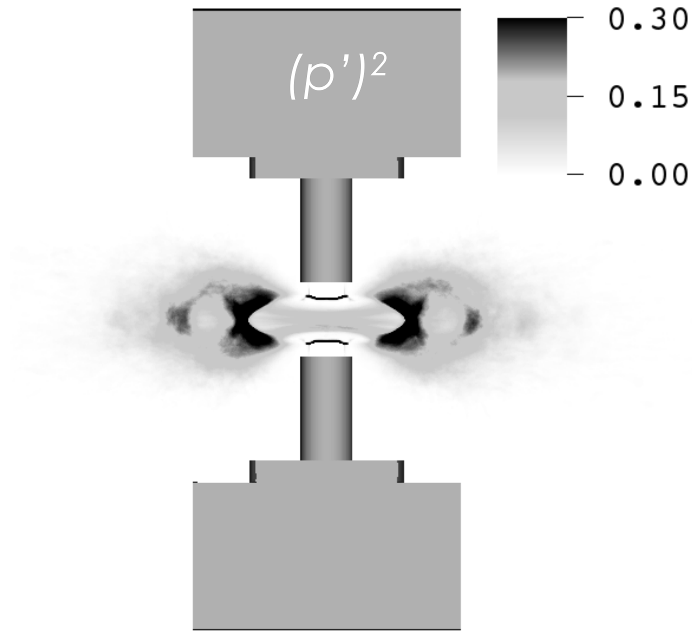

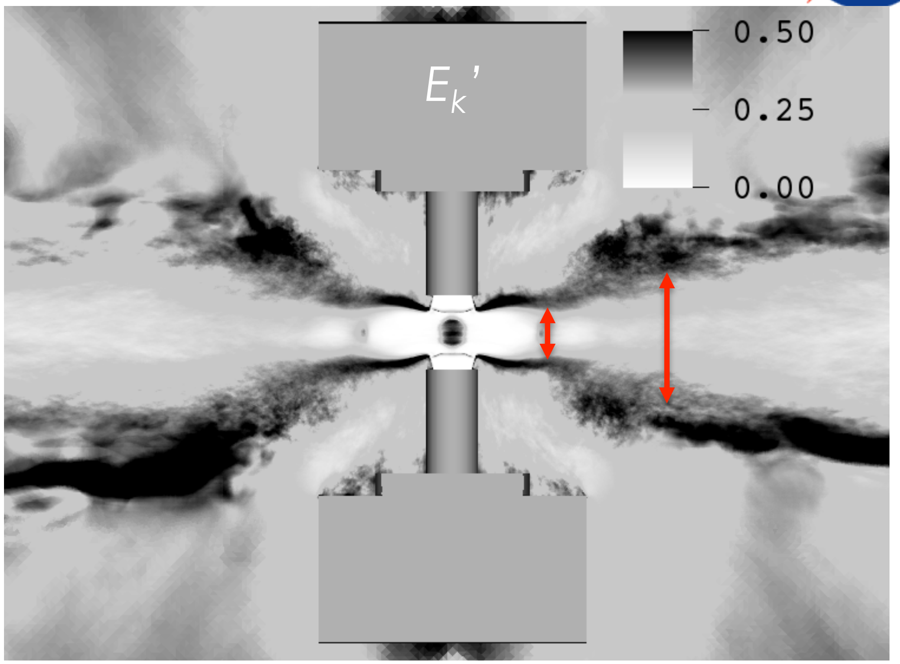

- Intermittency around the Mach disk of the first shock cell
- Intermittent motion of plate shocks of four jet impingement region
- Turbulent kinetic energy highlights shear layer and center of jet impingement region

➢ Turbulent kinetic energy seems to be more intermittent than disturbance pressure

Outline

- Introduction to BENS Aero-Acoustic Analysis
- Computational Simulation Strategy and Setup
- Characterization of Flow Field in Source Region
- **Noise Source Identification**
- Linear Acoustic Analysis
  - Acoustic Model of FJID
  - BENS Scattering Results
- Conclusions/Outlook

Causality Method to identify Noise Sources

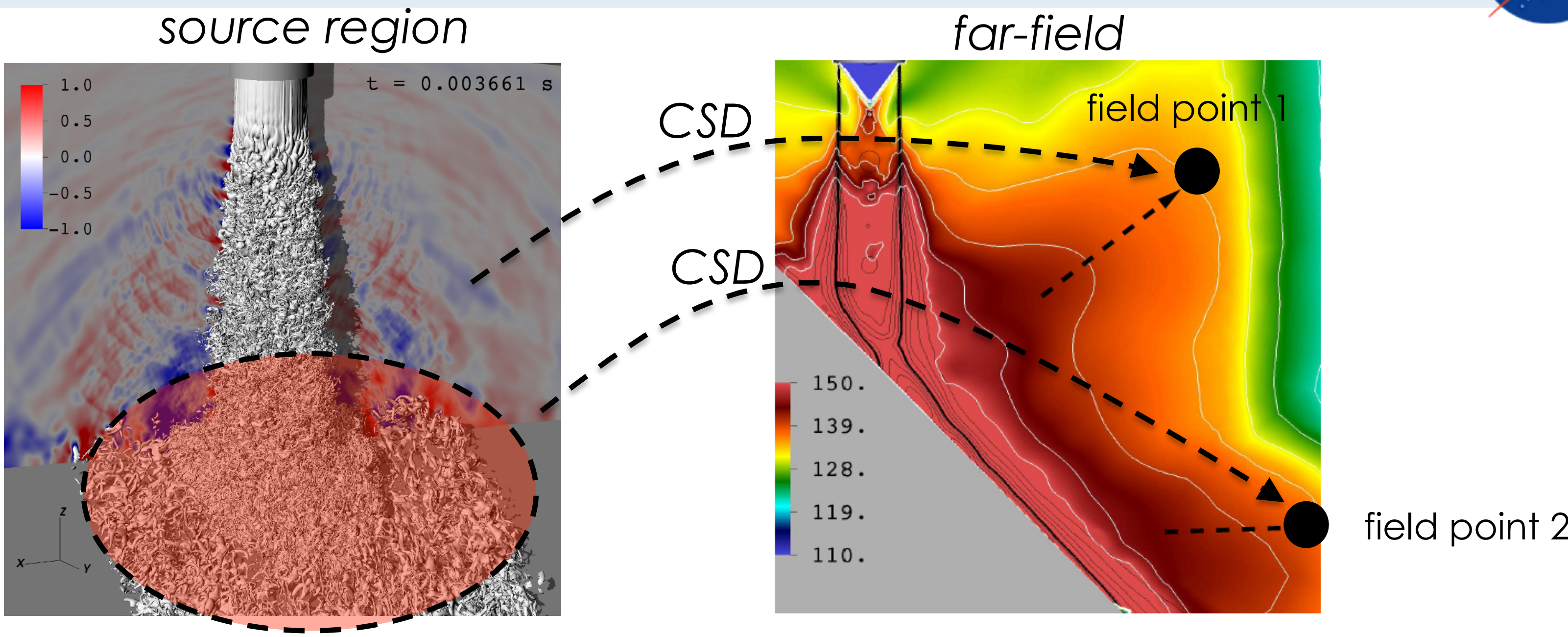

- Starting point Lighthill's acoustic analogy:

$$PSD_{p'}(\boldsymbol{x}_f, f) = -\frac{\pi f^2}{r a_\infty^2} \int_V CSD_{T_r,p'}(\boldsymbol{x}_f, \boldsymbol{x}_s, f) dV$$ (details in Brehm *et al.* [2015])

- Use normalized and un-normalized correlations
- Obtain link between source region and acoustic field
- Evaluate cross-spectral density (CSD) in entire plane of CFD data (difficult to achieve in experiment)
- Place field sensors in particular locations of interest, backtrack to source region and identify relevant flow physics

Following works by Proudman ('52), Rackl ('73), Hurdle ('74) , Goldstein ('75, '82, etc.), Krothapalli et al. ('99), Freund et al. ('01), Panda & Seasholtz ('02), Panda ('05), Bogey at al. ('07), Tam et al. ('08), Liu ('12,'14), Brehm at al. (2015) etc.

Normalized Cross-Correlations

Field Point 1

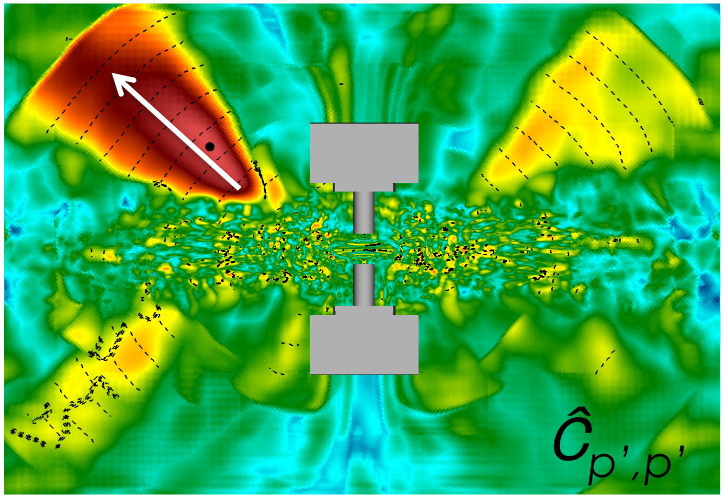

Field Point 2

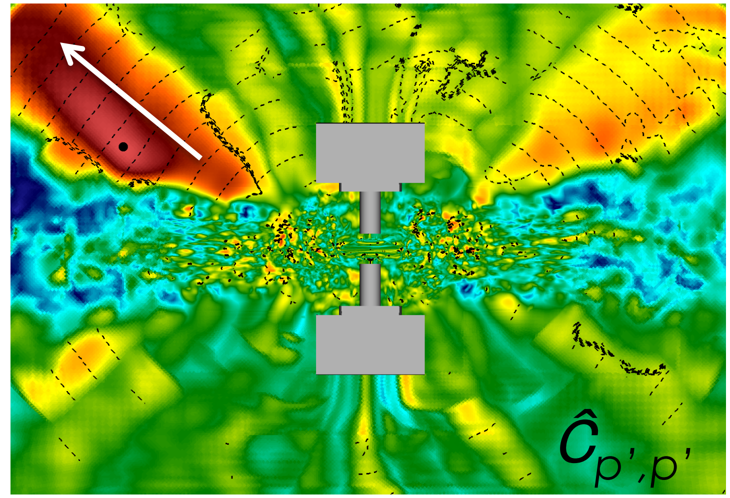

Field Point 3

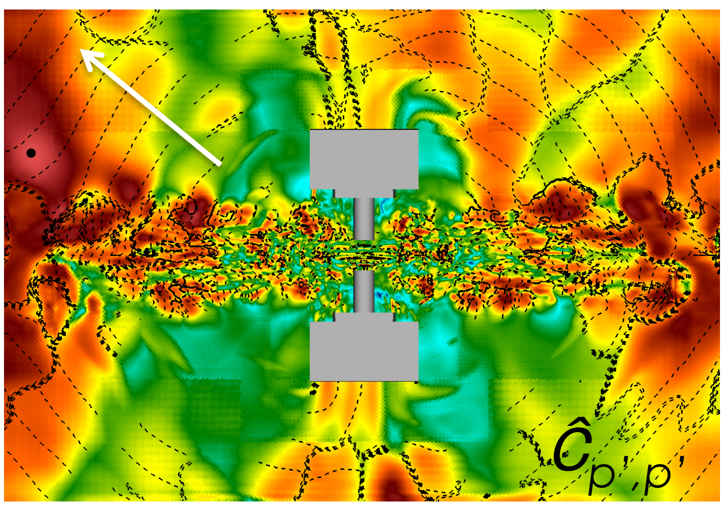

- Normalized peak correlations for different field points indicate that dominant noise sources are located in the break-up region of the deflected jets
- Cannot identify coherent flow structures that correlate well with p’
- Similar observation for $\hat{C}_{s',p'}$ and $\hat{C}_{Vr',p'}$

Causality Method Applied to FJID

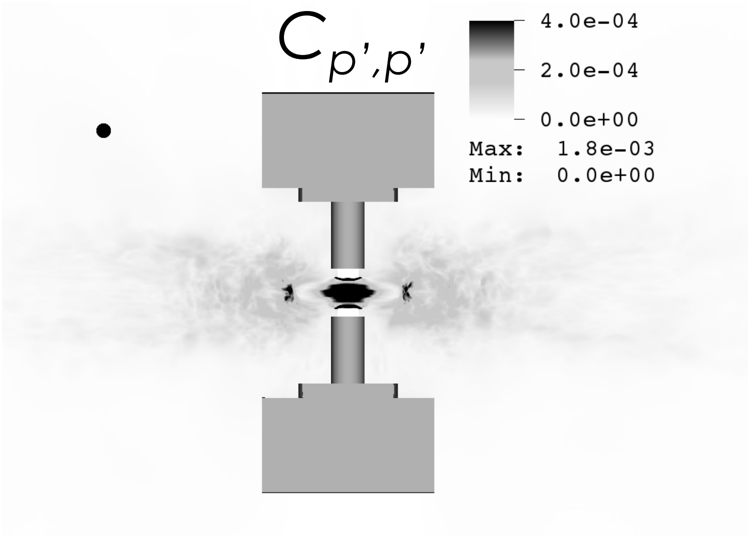

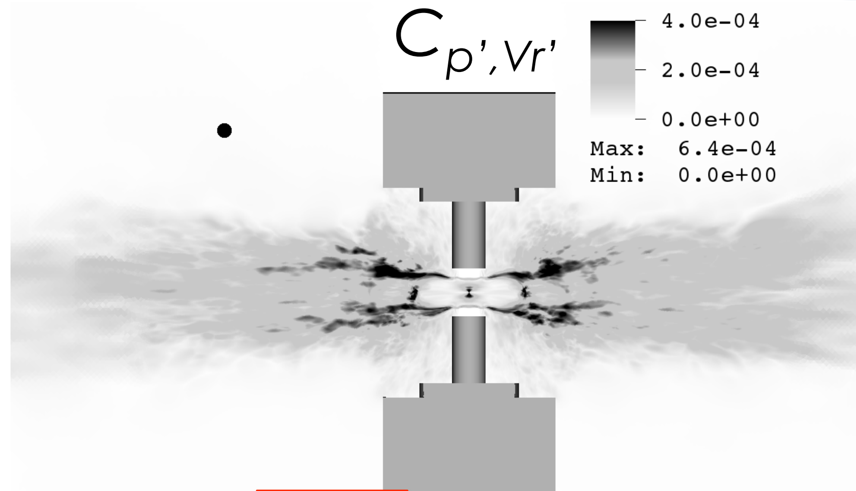

$$T_{ij} = \boxed{\rho u_i u_j} + \delta_{ij}(p - a_\infty^2 \rho)$$

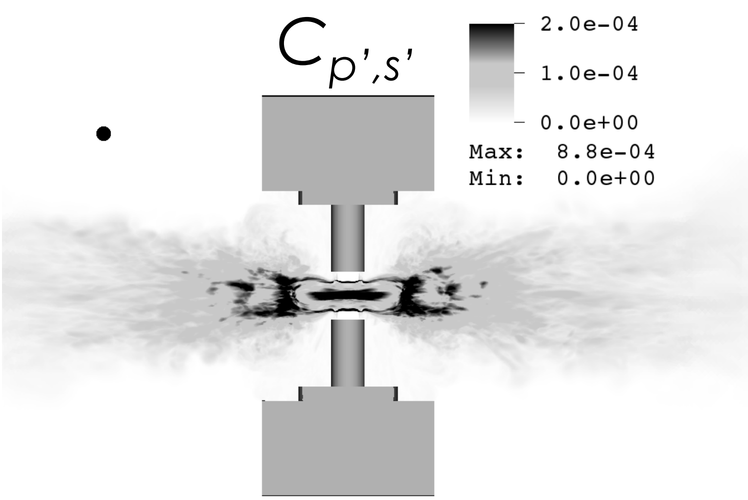

$$T_{ij} = \rho u_i u_j + \boxed{\delta_{ij}(p - a_\infty^2 \rho)}$$

Note: First order correlations only

- $C_{p',p'}$ displays large amplitudes in the impingement region and around normal shocks
- $C_{p',Vr'}$ highlights large fluctuations in the shear-layers
- $C_{p',s'}$ displays large amplitudes in the impingement region and around the first diamond shock structures

➢ Noise is generated in the direct vicinity of FJID (in intermittent flow regions)

Outline

- Introduction to BENS Aero-Acoustic Analysis
- Computational Simulation Strategy and Setup
- Characterization of Flow Field in Source Region
- Noise Source Identification
- **Linear Acoustic Analysis**
  - **Acoustic Model of FJID**
  - BENS Scattering Results
- Conclusions/Outlook

Linear Acoustic Model of FJID

Simple linear acoustic model

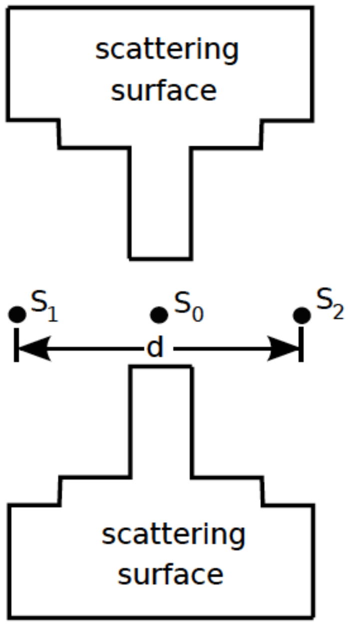

- Focus on single frequency St≈0.2; corresponds to peak frequency for turbo-machinery (~1.8kHz for full scale HWB)
- Develop a linear acoustic model that displays similar propagation pattern as CFD
- Test understanding of noise generation processes
- Previously FJID was thought of as an omni-directional noise source
- Different parameters: d, S_k, and phase relations
- Monochromatic/broadband noise source model

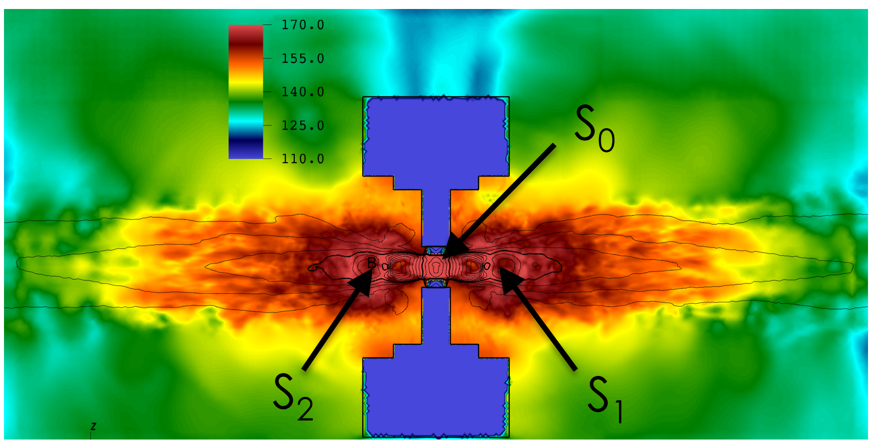

Sound pressure levels at St_C≈0.2 (1/3-octave band)

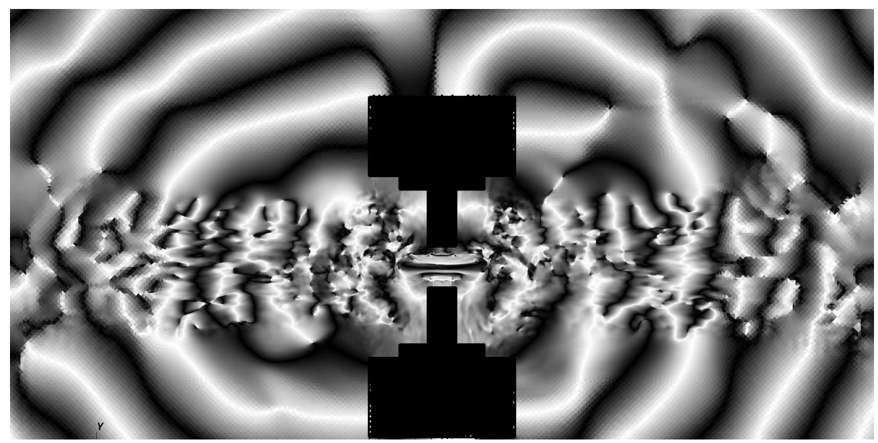

Phase plot at St≈0.2

Equivalent Source Method

- Helmholtz boundary value problem solver is key-component for ROM
- Solving: $\nabla^2 P' + k^2 P' = 0, \quad \forall \vec{x} \in \Omega; \qquad \frac{\partial P'}{\partial n} = -\hat{\imath} k \rho_\infty c_\infty \hat{u} \cdot \vec{n}, \quad \forall \vec{x} \in \partial\Omega;$

$$\lim_{R=|\vec{x}|\to\infty} \left[R \left(\frac{\partial P'}{\partial R} + \hat{\imath} k P' \right) \right] = 0$$ (Sommerfeld radiation condition)

  P' is acoustic pressure, k is the wavenumber, and ∞ refers to free-stream values

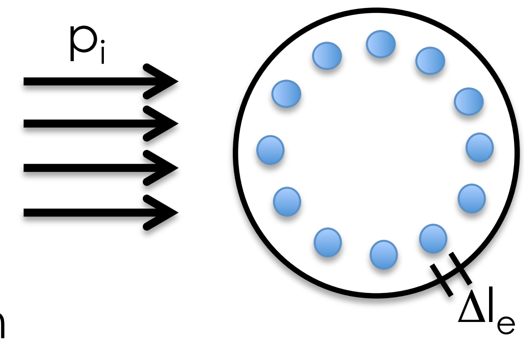

- Using free space Green's function
- Perfectly reflecting surface, $\hat{u} \cdot \vec{n} = 0$
- Radiating surface BCs
- Source region represented by monopole distribution
- M monopole sources are located inside radiating/scattering surface
- Solve over-determined system of equations for N triangles (M<N)

$$\left[\sum_{m=1}^{M} a_m \frac{\partial G(\vec{x}_n, \vec{x}_m)}{\partial n} \right] = -\hat{\imath} k \rho_\infty c_\infty \left[\hat{u} \cdot \vec{n} \right] (\vec{x}_n) \quad \text{for} \quad n = 1, \cdots, N$$

- MPI-parallel

see also Housman et al. (2013) and Kiris et al. (2014)

DEPENDENCE OF DISTANCE BETWEEN S_1 AND S_2

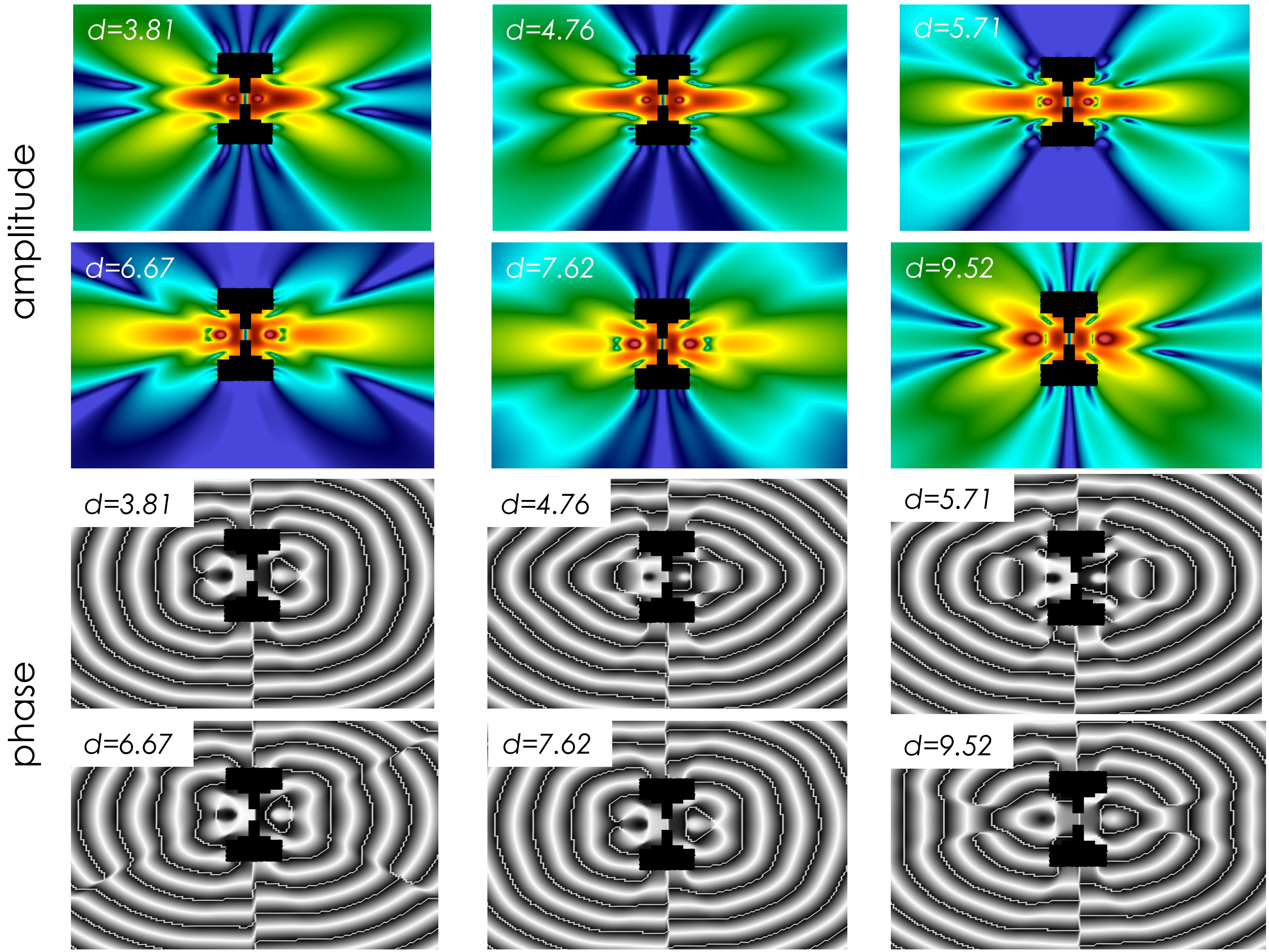

Dependence of distance between S_1 and S_2

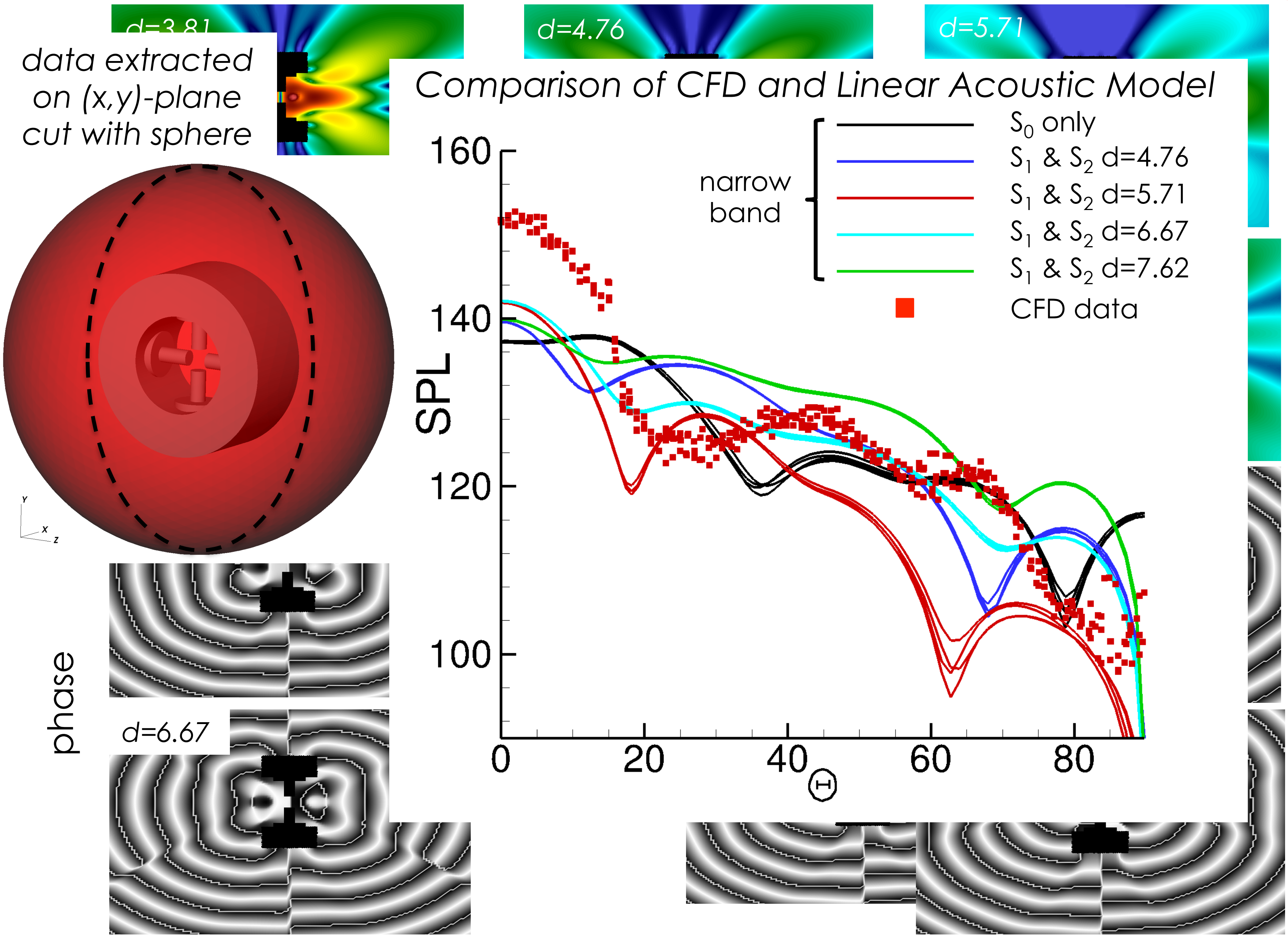

Broadband vs Monochromatic

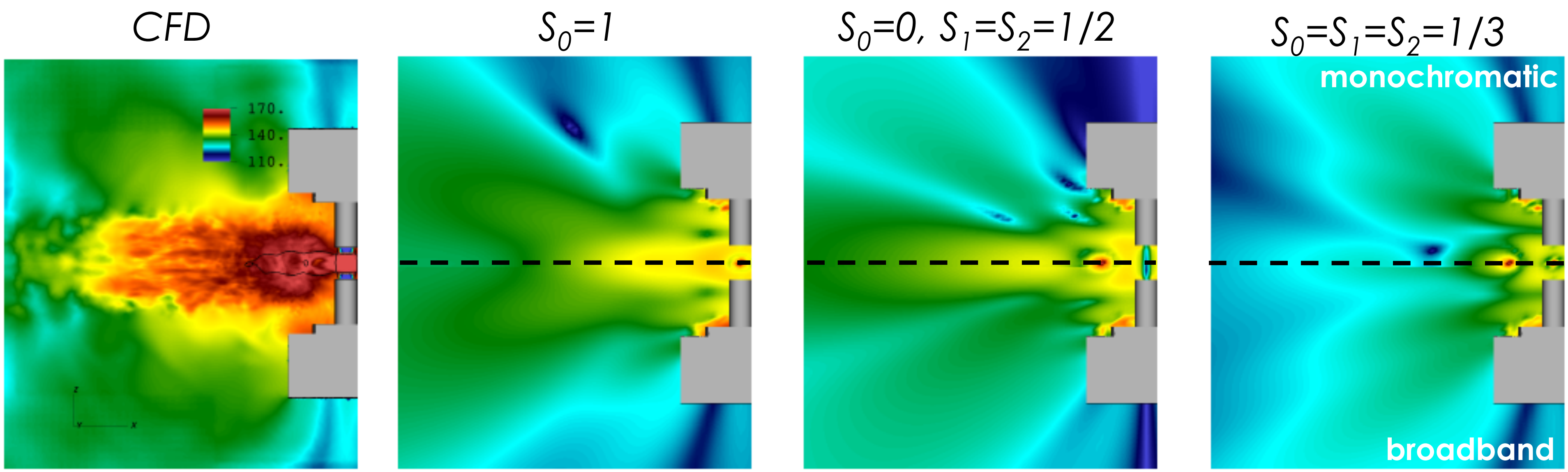

- Aim at modeling broadband noise in 1/3-octave bands
- Amplitude is fairly constant in octave-band centered around $St_C \approx 0.2$
- Monochromatic and broadband (white) noise sources are considered
- Amplitude relation: $A_{mono} = \sum_{n=1}^{N} A_{bb,n}^2$
- Unit amplitude for linear acoustic results (will be scaled based on CFD data)
- Parameter study to obtain correct parameters (S, d, and ϕ)
- Monochromatic and broadband results almost identical ($St/0.5\Delta St>8$)

Phase Plots

CFD | $S_0=1$ | $S_0=0,\ S_1=S_2=1/2$ | $S_0=S_1=S_2=1/3$

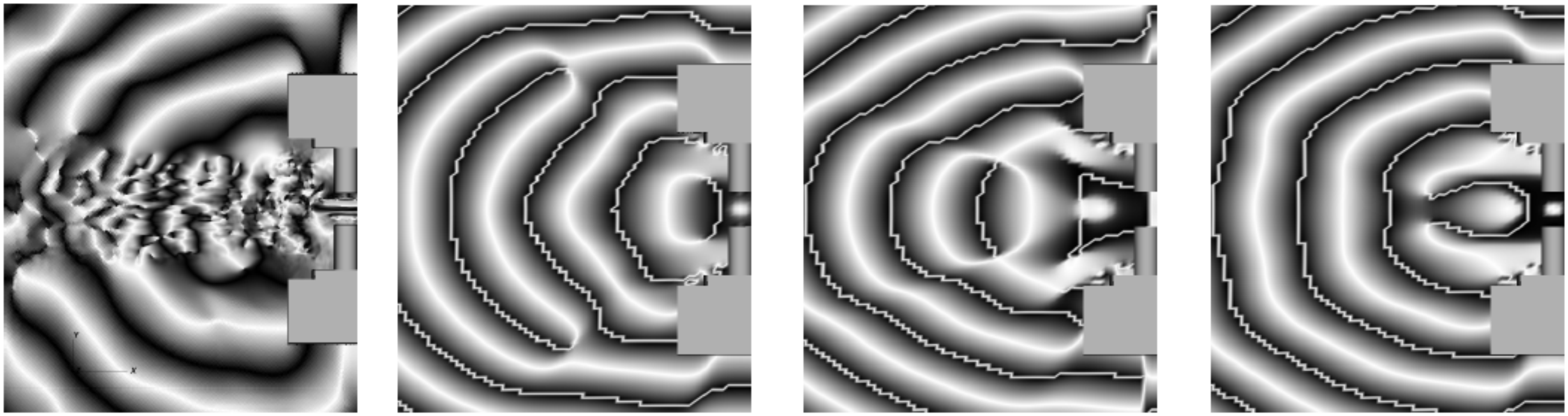

zero phase shift

- Wave fronts can be obtained from phase plots
- Phase plots mimic characteristics of CFD data
- Zero phase shift assumed for case 2 (not the case for asymmetric flapping jet)
- Cross-correlation function maximum for $\tau=0$ between left and right sides
- Phase relation between S_0 and S_1+S_2 is not clear

Most Promising linear Acoustic Models

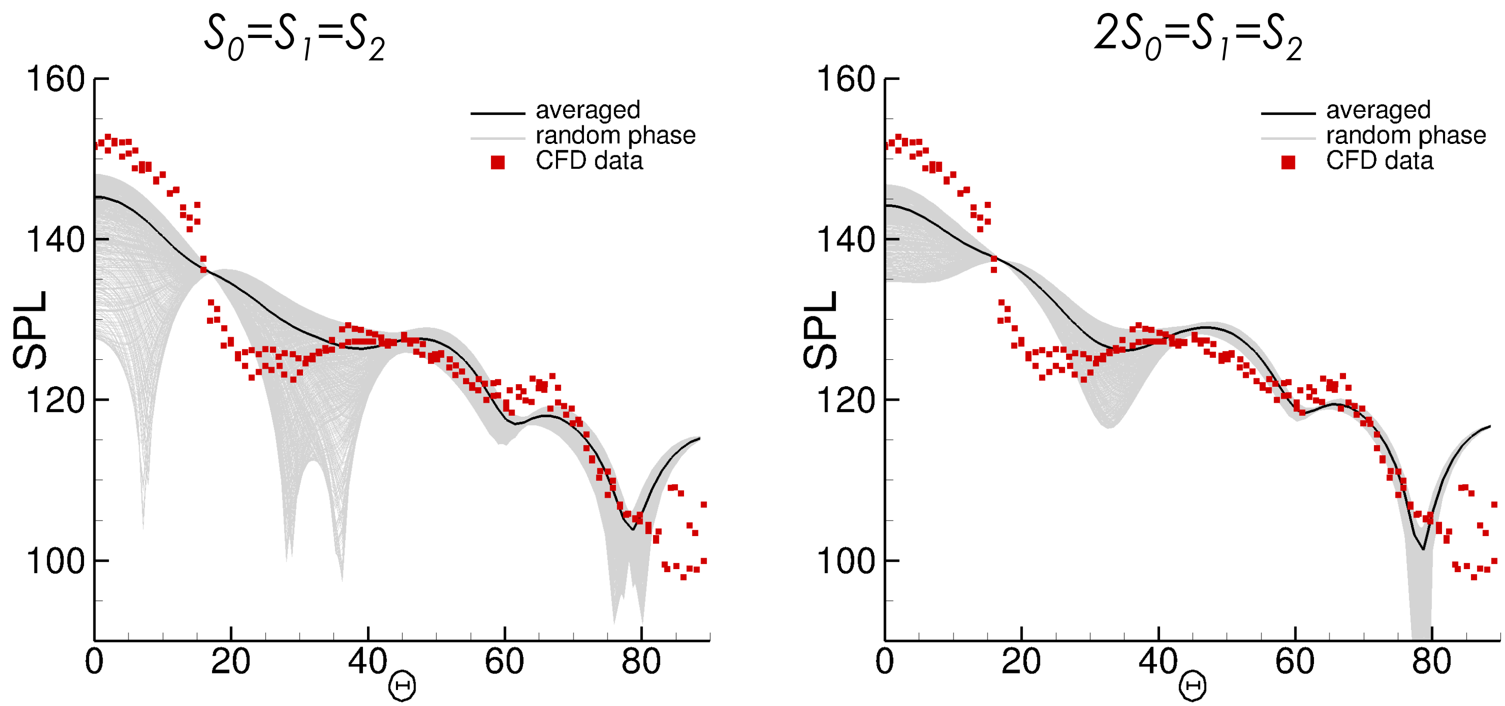

- Random phase result shown as solid black curve (average over grey curves)
- No meaningful comparison of SPL values for Θ in [0°,~20°] because CFD results are "polluted" with hydrodynamics pressure fluctuations
- Acoustic data does not account for refraction effects due to non-uniform mean flow
- Amplitude was scaled to match CFD
- Use acoustic model to simulate BENS experiment

OUTLINE

- Introduction to BENS Aero-Acoustic Analysis
- Computational Simulation Strategy and Setup
- Characterization of Flow Field in Source Region
- Noise Source Identification
- **Linear Acoustic Analysis**
  - Acoustic Model of FJID
  - **BENS Scattering Results**
- Conclusions/Outlook

Acoustic Scattering

- Place three dipole sources positioned at the center of each FJID (include scattering surface)
- Preliminary results computed at St≈0.2 (32 kHz) frequency
- Free-stream Mach number of zero (M≠0 will be considered later)
- Set-up is similar to that of Tinetti and Dunn AIAA-2012-2075, but includes plug and bracket geometry
- Fast turn-around time for design purposes (wall-clock time 20 minutes using 400 cores)
- Note that front is capped

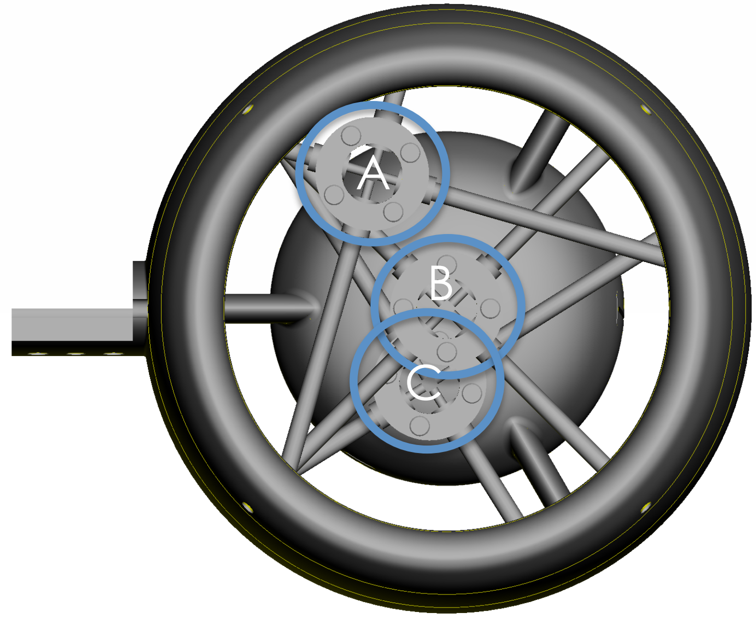

Utilize linear acoustic FJID model

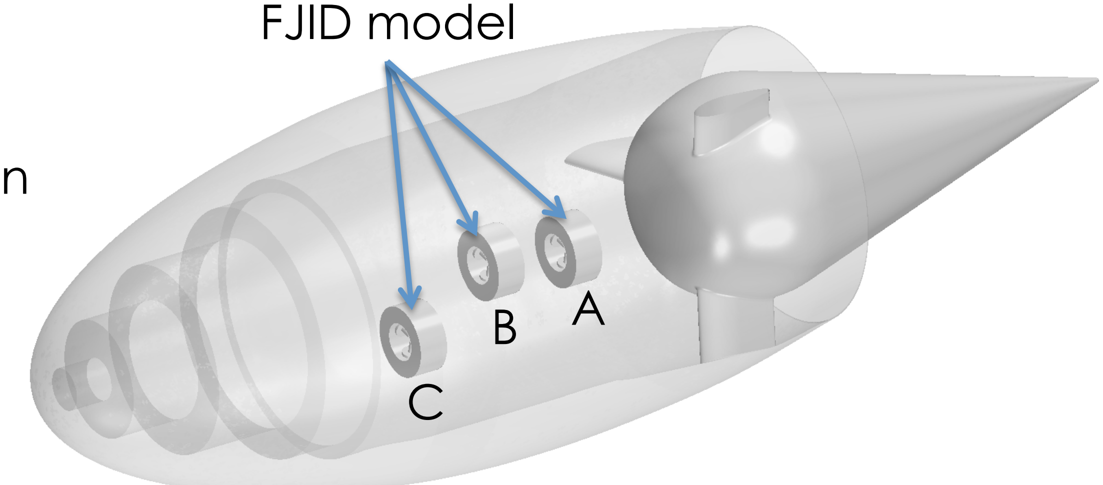

Acoustic Scattering

Solution Procedure (following Dunn & Tinetti):

(i) Run linear acoustic scattering code for FJID

- Using equivalent source method

(ii) Apply N=1000 random phases to each solution

- Parameter space (relative phases, ϕ_{12} and ϕ_{13}) generated with latin hypercube sampling

---

(iii) Superimpose 3 solutions and extract data on sampling line

- Average over all N samples

BENS containing 3 FJID models

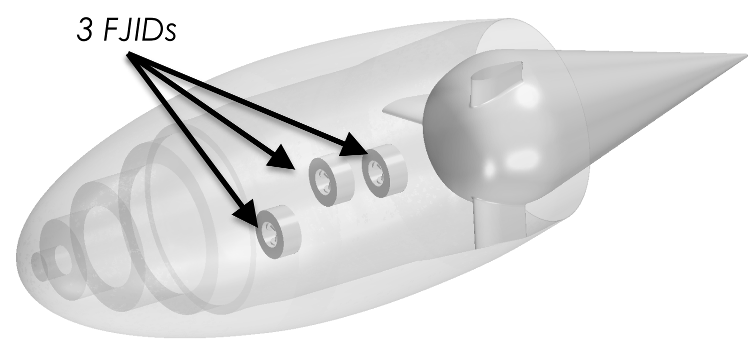

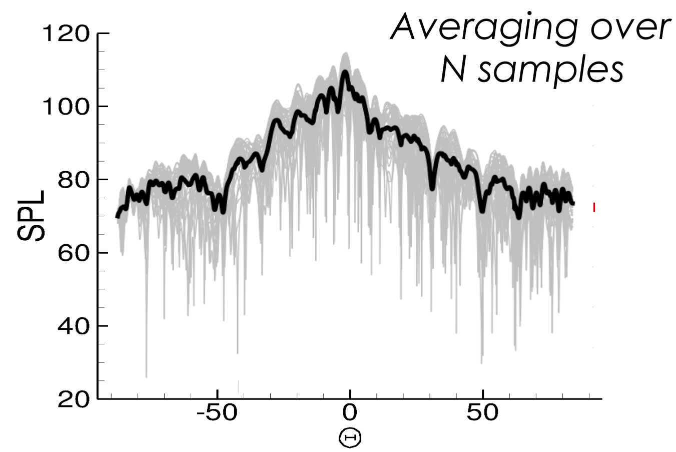

Extract data at specific locations

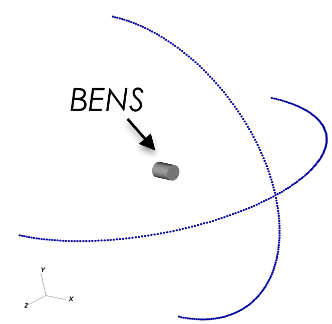

Acoustic Scattering

Conducted Sensitivity Studies:

- Offset distance
- Number of sources
- Resolution of scattering surface (5 ppw)
- Number of sample sets (phase & sub-intervals in octave band)

BENS with equivalent monopole sources

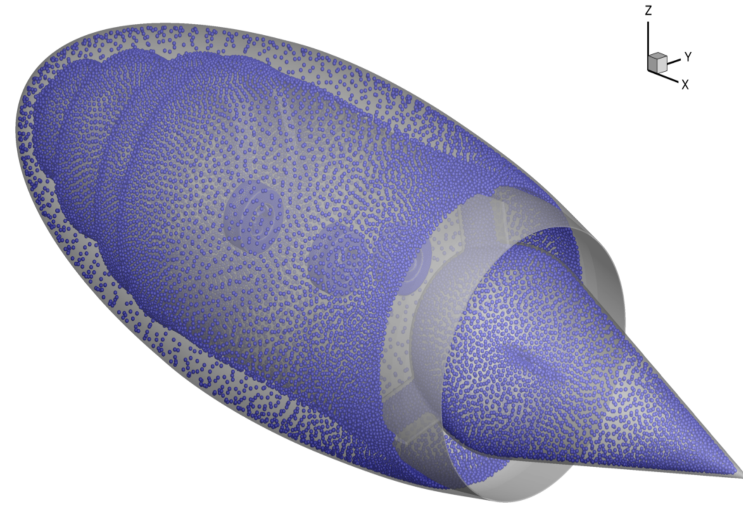

Comparison with experimental data:

FJID model + scattering surface

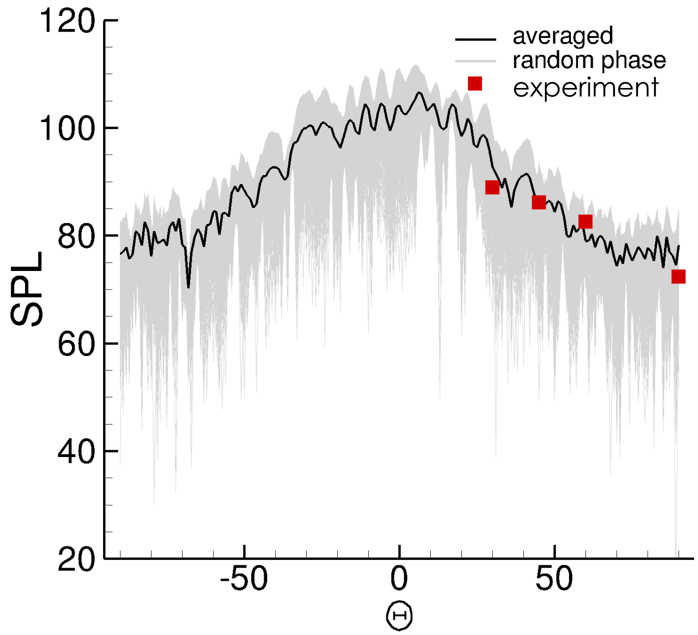

Single Monopole

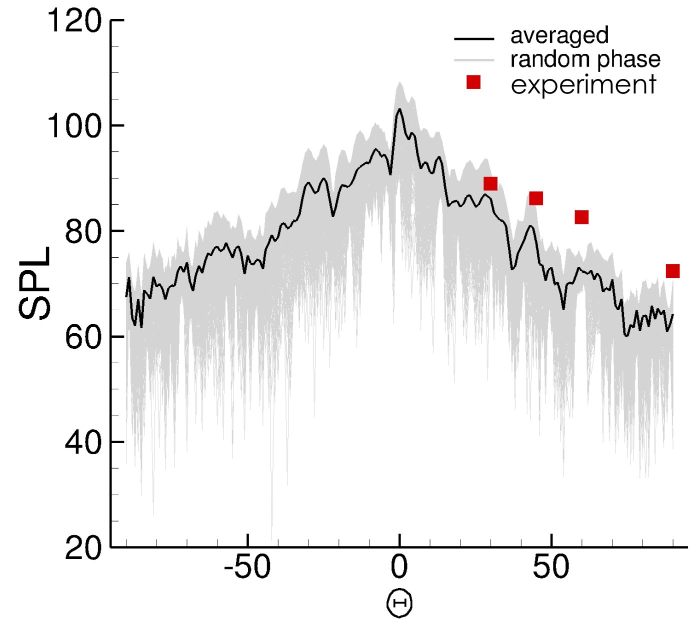

Outline

- Introduction to BENS Aero-Acoustic Analysis
- Computational Simulation Strategy and Setup
- Characterization of Flow Field in Source Region
- Noise Source Identification
- Linear Acoustic Analysis
  - Acoustic Model of FJID
  - BENS Scattering Results
- **Conclusions/Outlook**

SUMMARY

- Demonstrated the capability of noise source identification and characterization employing the causality method (and POD)

- Two key noise source mechanisms were analyzed
  - Shear layer interaction with first Mach cone diamond structure
  - Large entropy fluctuations within impingement region that is coupled to unsteady shock motion ➔ highly intermittent

- Development of linear acoustic model for four jet impingement device based on CFD results

- Good comparison of linear acoustic model with far-field measurement from BENS experiments

➢ Fully predictive capability of modeling the acoustic noise signature for BENS experiment (acoustic model solely based on CFD data)

Acoustic Scattering

Sound pressure level contours for full airplane linear acoustic scattering

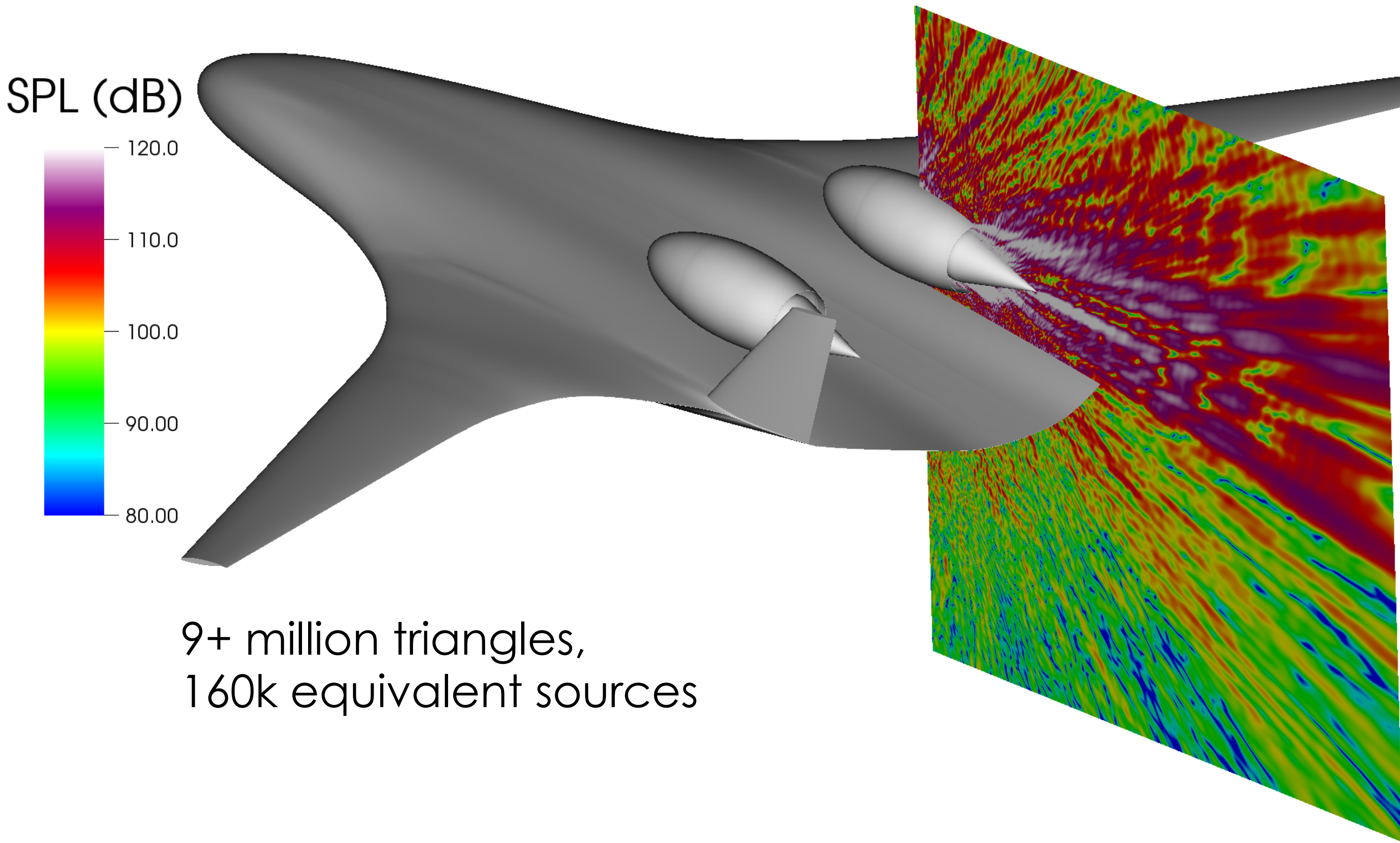

- Employ capability to conduct engine placement study for noise shielding
- Fast turn-around times allows for covering large design space
- In the next step, incorporate non-zero free-stream and refraction effects

Acknowledgement

- Thanks to **Russell Thomas**, **Christopher Bahr**, & **Casey Burley** from NASA Langley Research Center (LaRC) and **Kevin James** & **Mike Barad** from NASA Ames Research Center for valuable contributions
- Thanks to **Ted Manning** and **Emre Sozer** from NASA Ames Research Center (ARC) for their excellent feedback during ARC review process
- Work was funded by Environmentally Responsible Aviation (ERA) project
- Computer time was provided by NASA Advanced Supercomputing (NAS) facilities at ARC

Thank you for your attention!